Atmos. Meas. Tech. Discuss.,
doi:10.5194/amt-2017-323-AC1, 2017

Atmospheric Measurement Techniques Discussions

Interactive comment on "Error sources in the retrieval of aerosol information over bright surfaces from satellite measurements in the oxygen A-band" *by* Swadhin Nanda et al.

Swadhin Nanda et al.

nanda@knmi.nl

Received and published: 24 November 2017

Reviewer comment (general): This paper presents a comprehensive analysis on the potential error sources in aerosol height and optical thickness retrieval over different surface brightness. By breaking down the top of atmosphere reflectance into contribution from surface (Rs) and from the atmospheric column (Rp), the authors are able to analyze the mechanisms behind the potential retrieval bias/errors. The manuscript is organized and presented very well. It provides the community a detailed documentation on the problems facing aerosol property retrieval with oxygen A-band observations. I definitely recommend publication of the paper. I have several minor comments for the

authors to consider.

One general suggestion I have is to add some discussions on TOA reflectance sensitibity to layer height for optically thin aerosols. The manuscript uses thick aerosol layers (tau = 1.0) for this purpose (Figure 3 left panel). Since most aerosol layers are optically thin, a similar figure with aerosol optical thickness of 0.2 maybe more telling. I'm thinking a thinner layer would make the problem even harder.

Author's response: Thank you for your constructive feedback. The sensitivity studies in this paper were designed for the KNMI aerosol layer height algorithm, which primarily focuses on aerosol events with a UV absorbing index greater than 2. These are usually quite optically thick layers in the oxygen A-band. However, the question posed is a very valid one - How does the optical thickness determine the accuracy of retrieving aerosol layer height over bright surfaces?

To answer this, we have repeated the sensitivity analyses presented in Figure 7 (bottom left) for retrieval behaviour in the presence of model error in the surface albedo over a bright surface with a surface albedo 0.25 at 760 nm. The simulations are conducted for an aerosol optical thickness of 0.2, 0.5, 0.8 and 1.0. These are more realistic scenarios over Europe in terms of the presence of model errors and the amount of aerosols (see the plot in Figure 1). The caption of the figure is described as follows (the AMT online response editor's figure caption text box does not have enough space for the full caption):

'Bias in retrieved aerosol layer mid pressure (for different aerosol loads) versus introduced model error in the surface albedo relative to the truth (expressed in %) over a scene with a surface albedo of 0.25, viewing at a relative azimuth angle of 0°, solar zenith angle of 45°, and viewing zenith angle of 20°. The aerosols are represented by a single layer present at 650 hPa over a scene with surface pressure of 1013 hPa. The aerosols have a single scattering albedo of 0.95, and the scattering phase function is described by a Henyey-Greenstein model with an anisotropy factor of 0.7. The aerosol

optical thickness is described in the figure legend. Plot points represented with a cross represent non-convergences, i.e., no aerosol layer was retrieved in these cases. The bias is defined as the retrieved aerosol layer height minus the true aerosol layer height — a positive bias suggests that the retrieved aerosol layer is below the true aerosol layer.'

Optically thin aerosol layers will allow more photons to pass through and interact with the surface, leading to an increase in R_s, and hence an increase in the cancellation between R_p and R_s. With an increase in the aerosol optical thickness, less photons pass through the aerosol layer; consequently, biases in the retrieved aerosol layer height reduce as observed in Figure 1.

Changes to the manuscript: We will include the discussion presented here into the manuscript in Section 4.4 as a continuation from line 18 as - 'Retrieving height of optically thin aerosol layers can also be quite challenging, owing to the fact that these layers will allow more photons to pass through and interact with the surface, leading to an increase in R_s, and hence an increase in the cancellation between R_p and R_s. As a result of this, large biases in the retrieved aerosol layer height can be expected for optically thin layers over bright surfaces.'

Reviewer comment (specific 1): P8, Line 31: Figure 2 does show Rs is more significant than Rp, but that's for albedo = 0.4, not for a dark surface. Maybe just remove "(Figure 2, blue line)".

Author's response: Agreed.

Changes to the manuscript: Removed '(Figure 2, blue line)' from page 8, line 31.

Reviewer comment (specific 2): Figure 6: What would be the physical reasons for the

retrieval algorithm getting a positively biased optical thickness over brighter surfaces.

Author's response: The bias in the minimum of the cost function, in the case of Figure 6, need not be positive. It is also possible for this bias to be negative. In the calculation of the cost function (Equation 2 in the submitted manuscript), the synthetic measured spectrum **y** (or the 'truth' in this case) is at 600 hPa, whereas the modeled spectrum **F(x,b)** has an aerosol layer at 700 hPa. Because the aerosol layer in the modeled spectrum is lower than the same in the measured spectrum, the modeled atmospheric column that the photon passes through is longer, which increases the amount of absorption by molecular oxygen. Because of this, the aerosol optical thickness in the retrieval forward model is automatically adjusted (in this case, increased) in the minimum in order to compensate for the residual absorption. If the aerosol layer in the model is higher in the atmosphere than the same in the 'measured' (synthetic truth) spectrum, the minimum will appropriately shift to a lower value, in order to compensate for a deficit in the absorption in the spectrum generated by the retrieval forward model.

Changes to the manuscript: We have changed Page 9 line 9 (second paragraph) from 'Also, as Rs increases, the global minimum shifts away from the true τ. This is predominantly observed in Figure 6 (left, red line) over the bright surface for a viewing angle close to nadir, where R_s is more dominant. For the same angle, the global minimum over a dark surface is situated at the true τ value. As the viewing angle increases over the bright surface, R_p increases and the global minimum of the cost function moves closer towards the true τ.' to the following:

'Also, because of a model error (described in Figure 6) in the aerosol layer height between **y** and **F(x,b)**, (in Equation 2) the global minimum of the cost functions shifts away from the true τ. This shift is baised higher than the truth if the aerosol layer is lower in the atmosphere in comparison to the aerosol layer in the synthetic true spectrum, because the model has to compensate the extra absorption by molecular oxygen. If the aerosol layer is higher in the atmosphere, the minimum of the cost

function is situated at a τ lower than the true τ. As observed in Figure 6 (left, red line), this shift of the cost function minimum from the true τ is larger over bright surfaces for a viewing angle close to nadir, where R_S is more dominant. For the same angle, the global minimum over a dark surface is situated at the true τ value, even with the presence of a model disagreement with the simulated 'true' spectrum. As the viewing angle increases over the bright surface, R_p increases and the global minimum of the cost function moves closer towards the true τ.'

Reviewer comment (specific 3): P11, Line 15: "larger over land than the over the ocean" may be "larger over land that over ocean".

Author's response: Agreed.

Changes to the manuscript: Page 11, Line 15: changed 'larger over land than the over the ocean" changed to 'larger over land than over ocean".

Interactive comment on Atmos. Meas. Tech. Discuss., doi:10.5194/amt-2017-323, 2017.

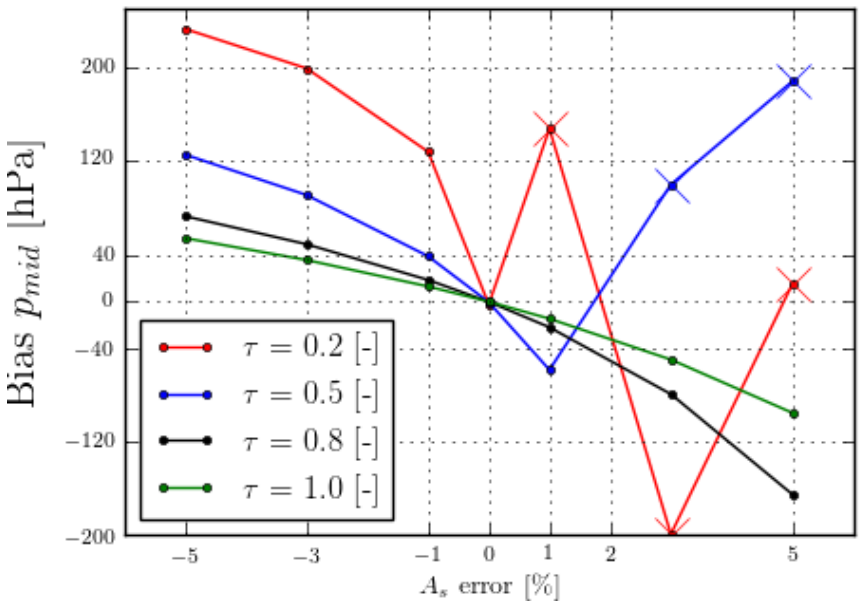

Fig. 1. Please check text for the caption.

Atmos. Meas. Tech. Discuss.,
doi:10.5194/amt-2017-323-AC2, 2017

Atmospheric Measurement Techniques Discussions

Interactive comment on "Error sources in the retrieval of aerosol information over bright surfaces from satellite measurements in the oxygen A-band" *by* Swadhin Nanda et al.

Swadhin Nanda et al.

nanda@knmi.nl

Received and published: 24 November 2017

Reviewer comment (general): The manuscript deals with the very challenging retrieval of aerosol height and amount from spectrally resolved satellite observations in the O2A band. An error characterization of a specific retrieval algorithm is presented and its capability is demonstrated in a case study. The topic is very relevant for a number of satellite instruments, the results are new and of interest to the community. Publication in AMT is recommended after the issues listed below are addressed.

The discussion of the mechanism leading to the near-singular regime (large retrieval uncertainties) is confusing. The authors should avoid talking about 'correlation of in-

formation', 'sign of information', and 'interference between light (contributions Rs and Rp)'. The discussing of the retrieval sensitivity based on the Jacobian (derivative of the top-of-atmosphere radiance R wrt z, AOT, SSA, Fig 4) and the cost function (Fig 6) is clear and instructive. It is not clear what exactly the separation into the derivatives of the contributions Rs and Rp add to this.

Author's response: Thank you for the constructive comments. Agreed that such terms can become confusing. These terms are appropriately changed and further discussed in the response to the second general comment. We will respond to your comment on our chosen method of explaining the retrieval problem using R_p and R_s.

The derivative of the reflectance with respect to model parameters is an important tool in understanding retrieval sensitivities. However, a general understanding of the change in the magnitude of the derivatives in Figure 4 with increasing surface albedo is, in our opinion, better explained as the interaction between R_p and R_s. This mathematical splitting of light into atmospheric path and surface contributions explains the reduction in the derivative of the reflectance to aerosol layer height with an increase in surface albedo at specific parts of the oxygen A-band spectrum (around 762 nm in Figure 4 top for instance) as a consequence of increasing R_s at the same spectral points. This also explains why the spectral shape of the derivative of the reflectance with respect of surface albedo becomes relatively more flat at approximately 0.25 surface albedo, with little variation between the continuum at 758 nm and the deepest part of the oxygen A-band in the R branch at 761 nm - the derivatives alone cannot explain why they change. We have, hence, chosen the splitting of top of atmosphere reflectance into individual atmospheric path and surface contributions as a tool to diagnose the variability of the Jacobian with change in model parameters.

Changes to the manuscript: Regarding the clarification of the manuscript with more appropriate terminology, we have made changes in-line with the response to the following reviewer general comment. We do not propose any changes regarding the second part of our response.

Reviewer comment (general): In many instances the formulations are creative (which is ok as such) but in some cases the clarity suffers. The manuscript needs to be checked and the clarity enhanced.

Author's response: We expect that with the proposed changes to the manuscript, the paper is more clear. As proposed by the referee, we will change some 'creative' terms in the manuscript with more apt describers. These are detailed in the following.

Changes to the manuscript: Page 1 Abstract, line 9 - changed 'The analysis shows that the information on aerosol layer height from atmospheric path contribution and the surface contribution to the top of atmosphere are opposite in sign' to 'The analysis shows that the derivative, with respect to aerosol layer height, of the atmospheric path contribution to the top-of-atmosphere reflectance is opposite in sign to the same of surface contribution - ...'

Page 7 line 14 - changed 'the difference spectra ...' to 'the difference spectrum'

Page 7 line 19 - changed 'it reveals an interference between these two contributions to the top of atmosphere reflectance' to '$\Delta R_{\Delta x}$ reduces following Equation 7, which may ...'

Page 7 line 28 - changed 'and hence an increase in interference between ...' to 'and hence an increase in cancellation between $\Delta R_{p\Delta z}$ and $\Delta R_{s\Delta z}$.'

Page 8 line 1-2 - changed 'Albeit subtle, the consequence of interference between ...' to 'Albeit subtle, the consequence of this cancellation between $\Delta R_{p\Delta z}$ and $\Delta R_{s\Delta z}$'

Page 8 line 7 - changed 'The interference between $\Delta R_{p\Delta \tau}$ and $\Delta R_{s\Delta \tau}$' to 'This anti-correlation'

Page 10 line 2-3 - changed 'This is explained by the lowered interference between R_p and R_s (Figure 2, red line). This is why the difference in errors between retrievals over the different surfaces reduces with an increase in viewing zenith angle' to 'This is explained by a reduction in R_s and an increase in R_p, (Figure 2, red line), which

explains why difference in errors between retrievals over different surfaces reduces with an increase in viewing angle (Figure 7, top left, high viewing zenith angles)'.

Page 10 line 10-26 - changed 'While it would appear that somehow the sensitivity of the retrieval to aerosol layer thickness increases with increasing surface albedo, this behaviour is explained better as perhaps the most interesting consequence of the interference between R_s and R_p ingrained within the optimal estimation framework. ... appear to have more absorption for observations over high surface albedos, corresponding to an aerosol layer closer to the surface than the true aerosol layer height' to 'This should not suggest a sensitivity to the geometrical thickness of the aerosol layer. As the surface albedo increases, the number of photons that pass through the atmosphere to interact with the surface before reaching the detector increases. These photons have a longer path length, which results in an increased absorption by oxygen at specific spectral points with weak oxygen absorption lines. In comparison to photons at wavelengths with strong oxygen absorption lines, these photons have a higher SNR, since relatively more of them reach the detector. A higher SNR ensures lower noise, and hence a higher value in the measurement error covariance matrix S_ϵ. If a spectral point has a higher value in S_ϵ, it has a higher representation in the cost function (in Equation 2), and hence a higher preference (or weight) in the optimal estimation. Because of this, the retrieval prefers to retrieve an aerosol layer height described by photons that travel through the aerosol layer closer to the surface. If, however, the aerosol optical thickness is so large that the photons cannot penetrate the aerosol layer, the retrieved aerosol layer height would be more accurate.'

Page 10 line 27 - Changed 'in the presence of interference between R_p and R_s' to 'over bright surfaces'

Page 11 line 8-9 - changed 'This again attributed to the decreased interference between R_p and R_s with increasing viewing angle' to 'This is again attributed to the decrease in R_p and increase in R_s with increasing viewing angle'.

Page 13 line 5 - please check response to minor comment 18

Page 15 line 8 - 'There exists an interference between scattered light by aerosols and the surface to the top of atmosphere reflectance in the oxygen A-band' changed to 'Depending on the surface brightness, the interaction of photons scattered from the atmosphere and the surface can result in a possible reduction of available aerosol information in the oxygen A-band spectrum.'

Page 15 line 10-11 - changed 'These interferences are dominant in high surface albedo regimes and viewing geometries close to the nadir' to 'The reduction of aerosol information increases with increasing surface brightness and decreasing viewing angle'

Page 15 line 11-12 - removed 'A consequence of this interference is a reduction in the amount of information the oxygen A-band spectra has on aerosol parameters.'

Page 15 line 12 - changed 'Our analyses reveal that the information available on aerosol optical ...' to 'Our analyses reveal that the derivatives of the atmospheric path and surface contributions with respect to ...'

Page 15 line 18 - 'since the interference between R_p and R_s reduces' changed to 'since R_p increases and R_s decreases'

Page 15 line 24-25 - 'with low absorption by oxygen have interference between R_p and R_s (see Figure 3, left), which are primarily prevalent over bright surfaces (such as land).' changed to 'with a low absorption by oxygen have an increased cancellation of $\Delta R_{p\Delta z}$ and $\Delta R_{s\Delta z}$ (see Figure 3, left) and hence a reduction in aerosol layer height sensitivity in specific parts of the spectrum (see Figure 4, top). This increases as surface albedo increases.'

Page 15 line 25-26 - 'It is also observed that the information content available on aerosol single scattering albedo (ω) in R_p and R_s are positively correlated' changed to 'it is also observed that the derivative of $\Delta R_{p\Delta\omega}$ and $\Delta R_{s\Delta\omega}$ are both positive (see Figure 3, right)'

Page 15 line 29 - changed 'This interference of R_p and R_s ' to 'The interaction between photons scattering back from the atmosphere (R_p) to the detector and photons that travel through the atmosphere to the surface to the detector (R_s)'

Page 15 line 31 - changed 'The interference of R_p and R_s ' to 'The sign difference of $\Delta R_{p\Delta\tau}$ and $\Delta R_{s\Delta\tau}$'

Page 16 line 8 - Removed 'This is, again, a consequence of the interference between R_p and R_s '

Reviewer comment (minor 1): Page 1 line 22 typo: if an aerosols

Author's response: Accepted.

Changes to the manuscript: Changed Page 1 line 22 'if an aerosols' to 'if aerosols'

Reviewer comment (minor 2): 2. Page 2 line 10: CALIPSO coverage area is not 'reduced' but maybe 'limited'

Author's response: Accepted.

Changes to the manuscript: Changed Page 2 line 9-10 from 'However, because of the limited swath of a space-borne lidar instrument, the mission coverage area is significantly reduced' to 'However, because of the limited swath of a space-borne lidar instrument, the mission coverage area is also limited'.

Reviewer comment (minor 3): Page 3 line 6: 'non-consequential' $>$ 'not affected'

Author's response: Accepted.

Changes to the manuscript: Page 3 line 6 'non-consequential' changed to 'not af-

fected'.

Reviewer comment (minor 4): Page 3 line 13-14: 'the cause of these errors needs to be extended' $>$ 'the concept of critical albedo needs to be extended'

Author's response: Accepted.

Changes to the manuscript: Page 3 line 13-14 'the cause of these errors needs to be extended' changed to 'the concept of critical albedo needs to be extended'.

Reviewer comment (minor 5): Page 5 line 3: formulation: 'due the wavelength band lying beyond' $>$ 'since the wavelength band is located beyond'

Author's response: Accepted.

Changes to the manuscript: Page 5 line 3 'due the wavelength band lying beyond' changed to 'since the wavelength band is located beyond'.

Reviewer comment (minor 6): Page 5 line 10: 'instead of the Henyey-Greenstein MODEL'

Author's response: Accepted.

Changes to the manuscript: Page 5 line 10 changed from 'instead of the Henyey-Greenstein' to 'instead of the Henyey-Greenstein model'.

Reviewer comment (minor 7): Page 5 line 18: 'the instrument's platform .. has been designed as a sounder' $>$ 'the instrument is a sounder'

Author's response: Accepted.

Changes to the manuscript: Changed page 5 line 18-19 'The instrument's platform has been designed as a geostationary atmospheric sounder with a hourly coverage' to 'The instrument is an atmospheric sounder on a geostationary platform with an hourly coverage'.

Reviewer comment (minor 8): Page 5 line 18: remove redundant information in 'The NEAR INFRARED spectrometer . . ., in the NEAR INFRARED.'

Author's response: Accepted with changes.

Changes to the manuscript: Page 5 line 20 changed 'The near infrared spectrometer has a FWHM of approximately 0.116 nm in the near infrared, oversampled by a factor of 3' to 'The instrument has a FWHM of approximately 0.116 nm, oversampled by a factor 3'.

Reviewer comment (minor 9): Page 6 line 6: provide justification for diagonality Page 6 line 16: It is wrong to state that the Jacobian is the primary reason for failure. It is singularity of the generalized inverse.

Author's response: Accepted.

Changes to the manuscript: Changed 'The matrices S_a and S_ϵ are diagonal, and are not correlated' to 'S_a is diagonal, assuming no correlation between state vector elements. S_ϵ is also diagonal, since the measurement error is assumed uncorrelated.'.

Page 6 line 15-17 'The Jacobian is also the primary reason why the retrieval can fail âĂŤ the Jacobian can become singular if the value of the partial derivative of the reflectance to the a state vector parameter is very low, or is correlated to another parameter in the state vector' changed to 'the Jacobian can become singular if the value of the partial

derivative of the reflectance to the a state vector parameter is very low, or is correlated to another parameter in the state vector.'

Reviewer comment (minor 10): Page 6 line 10: estimate . . . elements .. beyond boundary conditions $>$ beyond boundaries

Author's response: Accepted.

Changes to the manuscript: Page 6 line 21: 'the inverse method estimates state vector elements beyond their physical boundary conditions' changed to 'the inverse method estimates state vector elements beyond boundaries'

Reviewer comment (minor 11): Page 6 line 19: 'reveals interference between ΔR_p and ΔR_s' $>$ the increments can cancel.

Author's response: Accepted.

Changes to the manuscript: Please check response to main comment 2.

Reviewer comment (minor 12): Page 6 line 20: what is the 'relative difference'?

Author's response: In context to page 7 line 20, the line 'In such a case, the relative difference of ΔR_p and ΔR_s gives an idea on the magnitude of interference.' does not add to the paper very well. We will remove this line, in order to reduce any confusion/redundancy.

Changes to the manuscript: Page 7 line 20 removed 'In such a case, the relative difference of ΔR_p and ΔR_s gives an idea on the magnitude of interference'.

Reviewer comment (minor 13): Page 8 line 26: the root cause is the cancellation of the increments Delta_Rp and Delta_Rs (same spectral shape, same amplitude, opposite sign) rather than 'anticorrelation'.

Author's response: Accepted.

Changes to the manuscript: Changed Page 8 line 26 from 'due to the anti-correlation between ΔR_p and ΔR_s' to 'due to the cancellation between ΔR_p and ΔR_s owing to their similar amplitudes, spectral shapes but opposing signs.'

Reviewer comment (minor 14): Page 10 line 14/15: the retrieval sensitivity is not specific to any spectral point $>$ suggested to remove 'at that spectral point' in line 15.

Author's response: Accepted.

Changes to the manuscript: Removed 'at that spectral point' in page 10 line 15.

Reviewer comment (minor 15): Section 4.2. please mention which biases are discussed: bias in AOT or in z, or both?

Author's response: Section 4 discusses biases in the retrieved aerosol layer height. An extra line in the introduction to section 4 is added to clarify all subsequent mentions of 'biases'.

Changes to the manuscript: Section 4 Page 9 line 23-24 changed 'Error analysis is done for the aerosol layer height retrieval algorithm and a comparison is made between retrievals over ocean ...' to 'A comparative analysis of biases in the retrieved aerosol layer height is conducted over ocean ...'

Reviewer comment (minor 16): Page 11 line 1 typo: a biases cause by

Author's response: Accepted.

Changes to the manuscript: Changed Page 11 line 1 'The correlation of bias with surface albedo suggests that a biases cause by model ...' to 'The correlation of bias with surface albedo suggests that biases caused by model ...'

Reviewer comment (minor 17): Page 12 line 12/13: Are the terms 'a-priori' and 'first guess' used synonymously? (They should not.) Please report a-priori values for both parameters, or discuss why the first guess is important in this discussion.

Author's response: Accepted. Indeed this is a mistake on our part. The terms 'a-priori' and 'first guess' are not the same.

Also, the LER database used in the retrievals conducted in this paper are not on a 0.5° x 0.5° grid. Rather they are on a 1° x 1° grid.

Changes to the manuscript: Changed Page 12 line 10 'Surface albedo is derived using nearest neighbour interpolation from Tilstra et al. (2017), who provide monthly Lambertian Equivalent Reflectivity (LER) climatologies on a 0.5° x 0.5° grid' to 'Surface albedo is derived using nearest neighbour interpolation for version 1.3 of GOME-2A LER climatology derived from Tilstra et al. (2017), which is at a 1° x 1° grid'.

Changed Page 12 line 13 'In the inverse method, the first guess ...' to 'In the inverse method, the a-priori value ...'

Changed Page 13, Table 1 entry for 'surface albedo As' from 'GOME-2 LER at 0.5° x 0.5° grid at 758 nm and 772 nm' to 'GOME-2A LER at 1° x 1° grid at 758 nm and 772 nm'.

Reviewer comment (minor 18): Page 13 line 4-6: it is stated that the analysis and specifically Fig 7 top left explains the low bias of the retrieved layer height. This is not

understood. Please explain.

Author's response: Figure 7 (top left) provides examples of retrieving an aerosol layer of 50 hPa geometric thickness for a spectrum that represents an aerosol layer with a 200 hPa geometric thickness at an aerosol optical thickness of 1.0 at 760 nm. We observe that over higher surface albedos, the retrieved aerosol layer mid height is biased closer to the surface. Over a higher surface albedo, the contribution by R_s is also greater. These biases reduce significantly as the viewing zenith angle increases, which is also when R_s reduces (according to Figure 2). Since this is discussed in more detail in 4.1, we will mention a brief version of it in the changed version.

We observed, post submission, that the definition of bias in aerosol layer height mentioned in Page 9, line 25-26 is incorrect. This only applies to Figure 7 top left, and not to the rest of the sensitivity studies. For this we will include the correct figure (Figure 1) with the following caption

'Bias in aerosol layer height in the presence of model errors. Unless specified, the relative azimuth angle is 0° and the solar zenith angle is 45°, aerosol single scattering albedo of 0.95 and Henyey-Greenstein g of 0.7, and an aerosol layer at 650 hPa. **Top left**: Model error is introduced in the thickness of the aerosol layer. The simulated spectra contains a 200 hPa thick aerosol plume extending from the 1000 hPa to 800 hPa. **Top right**: Model error is introduced in the aerosol phase function. The simulated scenes contain aerosols with scattering physics described by a Henyey-Greenstein phase function with g = 0.65 and retrieved with g = 0.7. **Bottom left**: Model error is introduced in the single scattering albedo. The simulated spectra contains aerosols with ω = 0.95, which is fixed in the retrieval forward model at 0.90. **Bottom right**: A relative error is introduced in the surface albedo. The viewing angle is fixed at 20°.'

From these analyses, it is not straightforward to assume that the retrieved aerosol layer will be retrieved closer to the ground if surface albedo in the retrieval model is greater than the true surface albedo — this is not observed in Figure 6 bottom right for a surface

albedo of 0.25 and 0.4.

Changes to the manuscript: Changed 'From our analysis in Figure 7 (top left)' to 'This is explained by the increase in surface contribution R_s which represents photons passing through the atmosphere and interacting with the surface before reaching the detector. The spectral points representing these photons have a higher weight in the optimal estimation in comparison to the photons that do not interact with the surface and hence the aerosol layer height is retrieved closer to the surface.'

We propose to replace Figure 7 in the manuscript with Figure 1 proposed in this author's response. We also propose to replace Page 9 line 25-26 'Bias in the aerosol layer height is defined as the difference between true and retrieved aerosol layer height (in hPa) — a negative sign indicates that the aerosol layer is retrieved closer to the ground' with 'Bias in the aerosol layer height is defined as the difference between retrieved and true aerosol layer height (in hPa) — a positive sign indicates that the aerosol layer is retrieved closer to the ground with respect to the true aerosol layer height.'

Reviewer comment (minor 19): Page 14 line 29 (and Page 15 line 21) it is argued that there are multiple minima in the cost function, in case of high optical thickness. This finding should be presented in the body of the article before it is referred to in the discussion and in the conclusion.

Author's response: Section 3.2 Page 9, line 4 - 12 discusses the implication of surface brightness on the cost function. The general conclusion from Figure 6 is that the cost function can also contain multiple minima, one near the true aerosol optical thickness and one at a much higher value (Figure 6, left, slope after tau = 1.5). However, the figure presents only a single synthetic case of multiple minima over specific solar-satellite geometries. We understand that this can cause confusion in interpreting results presented in the paper. For that matter, we propose to remove the mention of multiple minima from Page 14 line 29. However, in Page 15, line 21, we refer to figure

6 (right), although not explicitly, where we see the cost function decreasing beyond the local minima close to the true aerosol optical thickness. To make this clear, we propose to mention Figure 6 (right) in this line, with the sentence made specific for the case presented in this figure.

Changes to the manuscript: Page 14 line 29 changed 'the retrieved aerosol optical thickness is typically beyond 4.0, for which we can expect multiple minima in the cost function' to 'the retrieved aerosol optical thickness is typically beyond 4.0.'

Page 15 line 20-21 changed 'We also notice the presence of multiple minima in the cost function for high aerosol optical thickness values' to 'We also notice that the cost function reduces at high aerosol optical thickness beyond the local minimum near the truth (Figure 6, right), which indicates the presence of multiple minima in the cost function.'

Reviewer comment (minor 20): Conclusion: please reformulate the discussion of interference and correlation of information.

Author's response: Accepted.

Changes to the manuscript: The following changes are also described in response to general comment 2.

Page 15 line 8 - 'There exists an interference between scattered light by aerosols and the surface to the top of atmosphere reflectance in the oxygen A-band' changed to 'Depending on the surface brightness, the interaction of photons scattered from the atmosphere and the surface can result in a possible reduction of available aerosol information in the oxygen A-band spectrum.'

Page 15 line 10-11 - changed 'These interferences are dominant in high surface albedo regimes and viewing geometries close to the nadir' to 'The reduction of aerosol information increases with increasing surface brightness and decreasing viewing angle'

Page 15 line 11-12 - removed ‘A consequence of this interference is a reduction in the amount of information the oxygen A-band spectra has on aerosol parameters.’

Page 15 line 12 - changed ‘Our analyses reveal that the information available on aerosol optical ...’ to ‘Our analyses reveal that the derivatives of the atmospheric path and surface contributions with respect to ...’

Page 15 line 18 - ‘since the interference between R_p and R_s reduces’ changed to ‘since R_p increases and R_s decreases’

Page 15 line 24-25 - ‘with low absorption by oxygen have interference between R_p and R_s (see Figure 3, left), which are primarily prevalent over bright surfaces (such as land).’ changed to ‘with a low absorption by oxygen have an increased cancellation of $\Delta R_{p\Delta z}$ and $\Delta R_{s\Delta z}$ (see Figure 3, left) and hence a reduction in aerosol layer height sensitivity in specific parts of the spectrum (see Figure 4, top). This increases as surface albedo increases.’

Page 15 line 25-26 - ‘It is also observed that the information content available on aerosol single scattering albedo (ω) in R_p and R_s are positively correlated’ changed to ‘it is also observed that the derivative of $\Delta R_{p\Delta\omega}$ and $\Delta R_{s\Delta\omega}$ are both positive (see Figure 3, right)’

Page 15 line 29 - changed ‘This interference of R_p and R_s ’ to ‘The interaction between photons scattering back from the atmosphere (R_p) to the detector and photons that travel through the atmosphere to the surface to the detector (R_s)’

Page 15 line 31 - changed ‘The interference of R_p and R_s ’ to ‘The sign difference of $\Delta R_{p\Delta\tau}$ and $\Delta R_{s\Delta\tau}$’

Page 16 line 8 - Removed ‘This is, again, a consequence of the interference between R_p and R_s ’

Interactive comment on Atmos. Meas. Tech. Discuss., doi:10.5194/amt-2017-323, 2017.

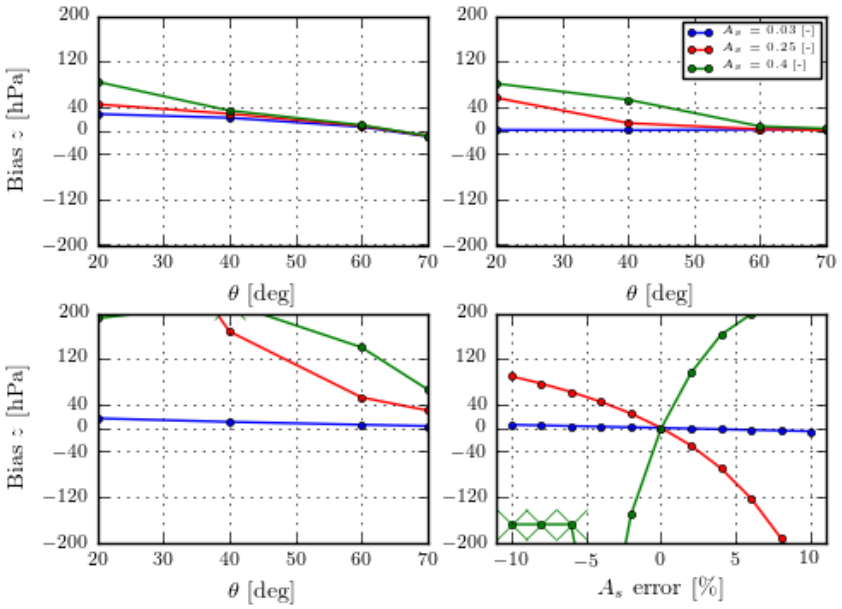

Fig. 1. Caption in text (response to minor 18)

Error sources in the retrieval of aerosol information over bright surfaces from satellite measurements in the oxygen A-band

Swadhin Nanda[1,2], Martin de Graaf[1], Maarten Sneep[1], Johan F. de Haan[1], Piet Stammes[1], Abram F. J. Sanders[3], Olaf Tuinder[1], J. Pepijn Veefkind[1,2], and Pieternel F. Levelt[1,2]

[1]Royal Netherlands Meteorological Institute (KNMI), Utrechtseweg 297, 3731 GA De Bilt, The Netherlands
[2]Delft university of Technology (TU Delft), Mekelweg 2, 2628 CD Delft, The Netherlands
[3]University of Bremen, Institute of Environmental Physics, Otto-Hahn-Allee 1, 28359 Bremen, Germany

Correspondence to: Swadhin Nanda (nanda@knmi.nl)

Abstract. Retrieving aerosol optical thickness and aerosol layer height over a bright surface from measured top of atmosphere reflectance spectrum in the oxygen A-band is known to be challenging, often resulting in large errors. In certain atmospheric conditions and viewing geometries, a loss of sensitivity to aerosol optical thickness has been reported in literature. This loss of sensitivity has been attributed to a phenomenon known as critical surface albedo regime, which is a range of surface albedos for which the top of atmosphere reflectance has minimal sensitivity to aerosol optical thickness. This paper extends the concept of critical surface albedo for aerosol layer height retrievals in the oxygen A-band, and discusses its implications. The underlying physics are introduced by analysing top of atmosphere reflectance ~~spectra~~ spectrum as a sum of atmospheric path contribution and surface contribution, obtained using a radiative transfer model. Furthermore, error analysis of ~~the~~ an aerosol layer height retrieval algorithm ~~are~~ is conducted over dark and bright surfaces to show the dependency on surface reflectance. The analysis shows that the ~~information on~~ derivative with respect to aerosol layer height ~~from~~ of the atmospheric path contribution ~~and the surface contribution to the top of atmosphere are~~ to the top-of-atmosphere reflectance is opposite in sign to the same of surface contribution — an increase in surface brightness results in a decrease in information content. In the case of aerosol optical thickness, these ~~contributions~~ derivatives are anti-correlated, leading to large retrieval errors in high surface albedo regimes. The consequence of this anti-correlation is demonstrated with measured spectra in the oxygen A-band from ~~GOME-2A~~ GOME-2 instrument on board the Metop-A satellite over the 2010 Russian wildfires incident.

1 Introduction

Aerosols are one of the largest source of uncertainties in our understanding of the Earth's current climate and its future projection, because of the role they play in complex atmospheric processes that influence the Earth's radiation budget (IPCC, 2014). More generally, aerosols influence the climate either directly through absorption and scattering of solar radiation, or indirectly through cloud formation and aerosol-cloud interaction.

In climate studies, the direct radiative effect of aerosols is calculated to understand its net contribution to the Earth's total radiation budget. This depends on aerosol macrophysics (such as vertical distribution) and microphysics (such as size distribution and single scattering albedo), which determine if aerosols in a particular scenario are more efficient in absorbing or

scattering the incoming solar radiation and the thermal radiation from within the Earth's atmosphere. The ability of aerosols to absorb radiation can influence thermal stability of the atmosphere, which in turn influences cloud formation and atmospheric chemistry (IPCC, 2014; Chung and Zhang, 2004). Knowledge on the vertical distribution on aerosols is, hence, an important piece of the puzzle to reduce uncertainties in our understanding of Earth's climate. Because of the high degree of variability of aerosols in both time and space, this knowledge is required at a high spatio-temporal resolution.

To observe (among other atmospheric parameters) aerosols, many space borne Earth observation initiatives have been proposed to monitor the Earth's atmosphere with either active or passive remote sensing techniques. An example of such an initiative is the Cloud-Aerosol LIdar with Orthogonal Polarisation (CALIOP) instrument on board NASA's Cloud-Aerosol Lidar and Infrared Pathfinder Satellite Observations (CALIPSO) mission, which provides information on the vertical distribution of aerosols. However, because of the limited swath of a space-borne lidar instrument, the mission coverage area is also limited. This gap in the data can be filled with satellite missions carrying passive remote sensing instruments, which have a larger coverage area with good temporal resolution. One such initiative is the Copernicus programme by the European Commission (EC) partnered with ESA, which aims to provide accurate information of atmospheric composition from space. Of its missions, the Sentinel-5 Precursor, Sentinel-5 and Sentinel-4 are examples of polar orbiting and geostationary satellites equipped with hyperspectral sensors (Veefkind et al., 2012; Ingmann et al., 2012).

Hyperspectral instruments on board the Sentinel-4/5/5P missions measure Earth radiance and Solar irradiance in the top of atmosphere, spectrally resolved over a wide wavelength range. Of the wavelength bands measured, these instruments also measure in the oxygen A-band between 758 nm and 770 nm where absorption of solar radiation is dominated by molecular oxygen and its isotopologues. The presence of aerosols in the atmosphere significantly impacts absorption of solar radiation by molecular oxygen (Figure 1, left). In the absence of clouds and aerosols, the oxygen A-band can either be almost transparent or opaque to solar radiation, owing to the large variation in the absorption cross section within the spectra. In the presence of an aerosol layer in the atmosphere, the absorption intensity of the spectra can provide useful vertical information (as observed in Figure 1, right) — deeper absorption lines correspond to a lower aerosol layer, shallow absorption lines for a higher aerosol layer. This is the basis of retrieving aerosol layer height from the oxygen A-band. Currently, the Copernicus Sentinel-4/5/5-P aerosol layer height algorithms are designed to exploit oxygen absorption spectra in the A-band to retrieve the height of an aerosol layer.

The retrieval of aerosol properties from the oxygen A-band presents a few challenges, one of them being that aerosol layers in the atmosphere are usually optically thin, and are quite difficult to observe in the presence of clouds. This is because clouds have an optical depth which is typically orders of magnitude larger than that of aerosols, and are more efficient in scattering incoming radiation. Consequently, aerosol retrieval algorithms generally refrain from retrieving over cloudy scenes; our algorithm is no exception to this and requires cloud screening to filter out pixels containing clouds.

While cloudy pixels can be filtered out to a certain degree, retrieving aerosols from measurements in the oxygen A-band over bright surfaces faces a host of other challenges. From literature, it is understood that aerosol information content from measured spectra in the oxygen A-band reduces as the surface albedo increases (Corradini and Cervino, 2006; Sanghavi et al., 2012). Sanders et al. (2015) report potentially large biases in their aerosol layer height retrievals from the oxygen A-band when

the surface albedo is fitted. In a previous paper, Sanders and de Haan (2013) also report that certain specific combinations of geometry, aerosol, and surface properties can result in unusually large uncertainties in the retrieved aerosol layer height (see also Figure 8-2 in Sanders and de Haan (2016)). Such large biases can perhaps be attributed to a phenomenon known as the critical surface albedo regime (Seidel and Popp, 2012), wherein for specific surface albedos, the top of atmosphere reflectance becomes independent of the aerosol optical thickness. Sanders et al. (2015) observe that when the surface albedo isn't fitted, typical uncertainties in the surface albedo database over land can result in large biases. From our analyses, we understand that for relative errors up to 10% in the surface albedo, retrievals over dark surfaces are not affected, whereas the same over sufficiently bright surfaces (surface albedo greater than 0.2) can suffer from very large biases.

A combination of all the error sources discussed previously can result in large biases. In fact, we observe that the presence of errors often lead to no convergence in the retrieval, with no concrete predictability on which pixel is likely to yield no result. Because of this, the operational algorithm wastes resources trying to retrieve aerosol layer height from pixels that potentially do not have any usable aerosol information. This is especially problematic in the framework of high resolution instruments, which demand operational processors to make efficient use of computational time and effort to process large number of spectra (typically several hundred per second). In order to design more efficient operational algorithms, the concept of critical surface albedo needs to be extended beyond the framework provided by Seidel and Popp (2012) into the oxygen A-band for aerosol optical thickness as well as aerosol layer height.

This paper analyses simulated measured top of atmosphere reflectance spectra in the oxygen A-band and provides an explanation for the loss of aerosol information over bright surfaces. Its implication is provided in an optimal estimation framework, specific to the retrieval of aerosol layer height, with results from sensitivity analyses. The analysis is followed up with a demonstration in a real data environment by retrieving aerosol layer height over a bright surface. The case study chosen is the retrieval of optically thick biomass burning aerosol plumes over the 2010 Russian wildfires, to demonstrate the effect of this loss of aerosol information over land. This paper is one in a series of papers on development of an operational oxygen A-band Aerosol Layer Height retrieval algorithm for Sentinel-4/5/5-P by KNMI, preceeded by Sanders and de Haan (2013) and Sanders et al. (2015). The current operational ALH algorithm for S5P is described in Sanders and de Haan (2016). While the results of this paper are relevant for the Sentinel 5-Precursor algorithm as well, the instrument model used in the sensitivity studies is for the UVN spectrometer on the S4 mission.

The next section (Section 2) provides a description of the forward model and the optimal estimation framework. Section 3 discusses the concept of aerosol-surface ambiguities in the oxygen A-band. Section 4 describes various sensitivities of our retrieval algorithm focusing on the difference between dark and bright surfaces. Section 5 discusses aerosol layer height retrievals over the 2010 Russian wildfires using GOME-2A data. Section 6 concludes this paper with a discussion and the implication of the findings from this paper.

2 The forward model and the inverse method

2.1 Forward model

There are three primary parts of the forward model, namely the the atmospheric model, the radiative transfer code, and the instrument model. A radiative transfer code is used to model a high resolution top of atmosphere radiance by propagating radiation through the atmosphere described by the atmospheric model. The top of atmosphere reflectance R computed by the forward model is defined as the ratio of the radiance I of the pixel measured by the instrument to the top of atmosphere solar irradiance E_0 of the pixel on a horizontal surface unit,

$$R(\lambda) = \frac{\pi I(\lambda)}{\mu_0 E_0(\lambda)}. \tag{1}$$

μ_0 represents the cosine of the solar zenith angle of the pixel, and λ represents the wavelength.

The top of atmosphere reflectance is calculated after the measured radiance and irradiance are convolved with the Instrument Spectral Response Function (ISRF) of the hyperspectral sensor in order to simulate measured spectra by a satellite instrument. For simulations, the high resolution solar ~~spectra by~~ spectrum from Chance and Kurucz (2010) is used.

2.1.1 Radiative transfer model

The radiative transfer model is the Layer Based Orders of Scattering (LABOS) method, which is a variant derived from the Doubling-Adding method (de Haan et al., 1987). Atmospheric properties are calculated line-by-line to compute the reflectance at the top of atmosphere. The radiative transfer code is a part of a software package called DISAMAR (Determining Instrument Specifications and Analysing Methods for Atmospheric Retrievals), which is the main workhorse of operational algorithm development efforts at KNMI for oxygen A-band aerosol height retrieval with S5P/S4/S5 instruments. Scattering by gases is described by Rayleigh scattering, which has a low scattering cross section in this wavelength region. Because of this, polarisation is ignored. Wavelength shifts caused by rotational Raman scattering (RRS) are ignored in order to reduce computational effort, since line by line calculations are computationally expensive in the oxygen A-band. This is convenient, since the Raman scattering cross section is even smaller than that of Rayleigh scattering. The atmosphere in the forward model is plane-parallel for the Earth radiance, and spherically corrected for the incoming solar irradiance.

2.1.2 Atmospheric model

For cloud-free conditions, the following four absorption and scattering processes are significant in the wavelength range between 758 nm and 770 nm: scattering by gases, reflection of light by the surface, scattering and absorption by aerosol particles, and absorption by molecular oxygen. Absorption of solar radiation by O_3 and H_2O are ignored, since they are not dominant absorbing gases in this spectral range.

The surface reflectance is assumed isotropic, described by its albedo. Depending on the surface albedo, a surface can either be bright or dark. Dark surfaces are classified with surface albedo close to 0.05 (or lower), which in the oxygen A-band spectral

region typically corresponds to ocean surfaces. Bright surfaces in the oxygen A-band on the other hand have a surface albedo of 0.2 (intermediately bright) and higher and are primarily over land. For the oxygen A-band at 760 nm, typical values of surface albedo over vegetated surfaces exceed 0.4 ~~due~~ since the wavelength band ~~lying~~ is located beyond the red edge where absorption of solar radiation by chlorophyll diminishes. Scenes with snow or ice are not processed.

Aerosols are represented as a single layer with a fixed pressure thickness of 50 hPa, containing aerosol particles with a fixed aerosol optical thickness and aerosol single scattering albedo. Aerosol layer height is defined as the mid-pressure of the aerosol layer — if the aerosol layer extends from 650 hPa to 600 hPa, the aerosol layer height is 625 hPa. In the operational S5P aerosol layer height algorithm, currently the aerosol phase function is a Henyey-Greenstein model (Henyey and Greenstein, 1941) with an asymmetry factor of 0.7, and an aerosol single scattering albedo of 0.95 (Sanders et al., 2015). While a Mie scattering model could be used instead of the Henyey-Greenstein model, the latter is computationally less expensive and hence more optimal for the operational algorithm.

Oxygen absorption cross-sections are derived from the NASA JPL database, following Tran and Hartmann (2008) who indicate that line parameters in the JPL database are more accurate than the HITRAN 2008 database. First-order line mixing and collision induced absorption by O_2-O_2 and O_2-N_2 are derived from Tran et al. (2006) and Tran and Hartmann (2008).

2.1.3 Instrument model

The instrument model is described by the instrument slit function, whose spectral resolution depends on its Full Width at Half Maximum (FWHM), and its noise model. For this study, oxygen A-band is simulated using specifications of the Sentinel-4 Ultraviolet Visible and Near infrared (UVN) instrument, which is set to launch in 2022. The instrument ~~'s platform has been designed as a geostationary atmospheric~~ is a sounder with a hourly coverage over Europe and Northern Africa at a spatial resolution of 8×8 km^2 sampled at 45°N and 0°E. The ~~near infrared spectrometer~~ instrument has a FWHM of approximately 0.116 nm~~in the near infrared~~, oversampled by a factor ~~of 3. Effectively, the~~ 3, effectively giving the instrument a spectral sampling interval of ~~the instrument is~~ 0.04 nm. Aerosol layer height will be an operational product provided by the Sentinel-4 mission. An example of oxygen A-band spectra at a 0.116 nm resolution is provided in Figure 1. For retrievals with real data, measurements from the Global Ozone Monitoring Experiment-2 on board the MetOp-A satellite are used. Launched on October 16, 2006, GOME-2A is an optical spectrometer fed by a scanning mirror which enables across-track scanning in the nadir. The instrument has a spectral sampling interval of approximately 0.21 nm at 758 nm (spectral resolution of 0.48 nm for channel 4), and has a nominal spatial resolution of 80×40 km^2 (Munro et al., 2016). ~~The noise model assumes a noise spectrum dominated by shot noise~~ A shot noise model is assumed for the instrument.

2.2 Inverse method

The inverse method is based on the Optimal Estimation (OE) framework described by Rodgers (2000), which is a Maximum A-Posteriori (MAP) estimator that constrains the least-squares solution with a-priori knowledge on the state vector. The method

assumes Gaussian statistics for the a-priori errors. The iterative method is a Gauss-Newton approach, and the estimation parameters are the aerosol optical thickness τ and the aerosol layer height z. The cost function χ^2 is defined as,

$$\chi^2 = [\mathbf{y} - \mathbf{F}(\mathbf{x}, \mathbf{b})]^T {\mathbf{S}_\epsilon}^{-1} [\mathbf{y} - \mathbf{F}(\mathbf{x}, \mathbf{b})] + (\mathbf{x} - \mathbf{x_a})^T {\mathbf{S_a}}^{-1} (\mathbf{x} - \mathbf{x_a}), \tag{2}$$

where $\mathbf{y}$ is the measured reflectance, $\mathbf{F}(\mathbf{x}, \mathbf{b})$ is the vector of calculated reflectance using the forward model, $\mathbf{x}$ is the state vector containing fit parameters, $\mathbf{b}$ is the vector containing other model parameters, $\mathbf{S}_\epsilon$ is the measurement error-covariance matrix, $\mathbf{x_a}$ is the a-priori state vector, and $\mathbf{S_a}$ is the a-priori error-covariance matrix. ~~The matrices~~ $\mathbf{S_a}$ ~~and~~ is diagonal, assuming no correlation between state vector elements. $\mathbf{S}_\epsilon$ ~~are diagonal, and are not correlated~~is also diagonal, since the measurement error is assumed uncorrelated. $[\mathbf{y} - \mathbf{F}(\mathbf{x}, \mathbf{b})]^T {\mathbf{S}_\epsilon}^{-1} [\mathbf{y} - \mathbf{F}(\mathbf{x}, \mathbf{b})]$ is the measurement part of the cost function, whereas $(\mathbf{x} - \mathbf{x_a})^T {\mathbf{S_a}}^{-1} (\mathbf{x} - \mathbf{x_a})$ is the ~~a-priori~~ state vector part of the cost function.

The a-posteriori error covariance matrix $\hat{\mathbf{S}}$ is computed as,

$$\hat{\mathbf{S}} = (\mathbf{K}^T \mathbf{S}_\epsilon \mathbf{K} + {\mathbf{S_a}}^{-1})^{-1}, \tag{3}$$

where $\mathbf{K}$ is the Jacobian with its columns containing partial derivatives of the reflectance with respect to the state vector elements. DISAMAR calculates the Jacobian semi-analytically, similar to the reciprocity method described by Landgraf et al. (2001). The Jacobian drives the retrieval towards the solution as an integral component in the update to the state vector,

$$\mathbf{x}_{n+1} = \mathbf{x_a} + ({\mathbf{K_n}}^T {\mathbf{S}_\epsilon}^{-1} \mathbf{K_n} + {\mathbf{S_a}}^{-1})^{-1} {\mathbf{K_n}}^T {\mathbf{S}_\epsilon}^{-1} [\mathbf{y} - \mathbf{F}(\mathbf{x_n}) + \mathbf{K_n}(\mathbf{x_n} - \mathbf{x_a})], \tag{4}$$

where $\mathbf{x}_{n+1}$ is the next iteration to the n^{th} iteration in the retrieval, and $\mathbf{K_n}$ is the Jacobian evaluated at the n^{th} iteration. The Jacobian ~~is also the primary reason why the retrieval can fail — the Jacobian can~~ can become singular if the value of the partial derivative of the reflectance to the a state vector parameter is very low, or is correlated to another parameter in the state vector. In these cases, the error covariance matrix does not exist, since the inverse covariance matrix is non-invertible; if it is *nearly* singular, the problem is ill-conditioned and may result in very large biases in the estimation.

The inverse method reaches a solution if the change in the state vector between iterations is below a convergence threshold. It is possible that during iterations, the inverse method estimates state vector elements beyond ~~their physical boundary conditions~~boundaries. In such a case, the state vector element is adjusted back to just within its physical limits. If the adjustment is made in two consecutive iterations, the retrieval is stopped and no solution is reached. The upper cap in the number of iterations is set at 12, beyond which the retrieval is said to have failed. In this paper, these failed retrievals are termed as non-convergences. The next section discusses the atmospheric conditions that can potentially lead to these non-convergences.

3 Aerosol-surface ambiguities in the oxygen A-band

3.1 Influence of surface reflectance on aerosol information content in the oxygen A-band

The top of atmosphere reflectance over a surface with an albedo A_s can be written as the sum of ~~photon path contribution~~ atmospheric path contribution of the photon R_p and surface contribution R_s,

$$R(\lambda, A_s) = R_p(\lambda) + R_s(\lambda, A_s). \quad (5)$$

R_p is the top of atmosphere reflectance in the absence of a surface. R_s is calculated by subtracting the path contribution from the total top of atmosphere reflectance, and represents contributions from photons that have been reflected one or more times by the surface. R_s is dependent on the absorbing and scattering species present in the atmosphere, and also includes aerosol influences. R_p is calculated by substituting $\mathrm{A}_s = 0.0$ and calculating the top of atmosphere reflectance in DISAMAR. R_s is calculated by subtracting R_p from R. With increasing viewing angle, R_p increases whereas R_s decreases (Figure 2). This is in line with expectation, since the slant aerosol optical thickness increases, which increases the amount of contribution that aerosols have in $R(\lambda, A_s)$. At steeper geometries, light at the top of atmosphere is more diffuse than direct, which is the primary reason why R_s decreases (assuming a Lambertian surface).

For a model parameter x with two values x_a and x_b, the difference ~~spectra~~ spectrum $\Delta R_{\Delta x}$, defined as

$$\Delta R_{\Delta x} = R_{x_a} - R_{x_b}, \quad (6)$$

can reveal the influence the model parameter x has on the oxygen A-band. The spectral shape of $\Delta R_{\Delta x}$ can also show parts of the spectrum that are more sensitive to x. Following Equations 5 and 6, $\Delta R_{\Delta x}(\lambda, A_s)$ is defined as

$$\Delta R_{\Delta x}(\lambda, A_s) = \Delta R_{p_{\Delta x}}(\lambda) + \Delta R_{s_{\Delta x}}(\lambda, A_s). \quad (7)$$

If $\Delta R_{p_{\Delta x}}$ and $\Delta R_{s_{\Delta x}}$ have opposing signs, ~~it reveals an interference between these two contributions to the top of atmosphere reflectance, which may result~~ $\Delta R_{\Delta x}$ reduces following Equation 7 which results in a reduction of sensitivity to the parameter x. ~~In such a case, the relative difference of the magnitude between $\Delta R_{p_{\Delta x}}$ and $\Delta R_{s_{\Delta x}}$ gives an idea on the magnitude of interference.~~

Comparing $\Delta R_{p_{\Delta z}}$ and $\Delta R_{s_{\Delta z}}$ at two different aerosol layer heights (z) for two different scenes with the same atmospheric conditions (Figure 3, left panel), it is observed that $\Delta R_{p_{\Delta z}}$ and $\Delta R_{s_{\Delta z}}$ have opposite signs and R_p is relatively more sensitive to aerosol layer height than R_s. This is especially the case in the deepest part of the R-branch between 759.50 nm and 761.30 nm and parts of the P-branch between 761.30 nm and 763.00 nm, where the higher absorption cross section reduces the number of photons that can reach the surface. This ultimately reduces the magnitude of R_s to the top of atmosphere for these absorption sub-bands. $\Delta R_{s_{\Delta z}}$ over ocean and vegetation also shows an increase in its overall magnitude with an increase in surface

albedo, and hence an increase in ~~interference between $\Delta R_{p_{\Delta z}}$ and $\Delta R_{s_{\Delta z}}$~~cancellation between $\Delta R_{p\Delta z}$ and $\Delta R_{s\Delta z}$. Figure 4 represents the variation of the derivative of reflectance with respect to aerosol properties, for increasing surface albedo. Albeit ~~sublte~~subtle, the consequence of ~~interference between $\Delta R_{p_{\Delta z}}$ and $\Delta R_{s_{\Delta z}}$~~ this cancellation between $\Delta R_{p\Delta z}$ and $\Delta R_{s\Delta z}$ is observed in Figure 4 (Top), where $\partial R/\partial z$ for the deepest part in the R-branch and parts of the P-branch diminishes gradually with an increase in surface albedo.

The same experiment is repeated for aerosol optical thickness (τ), and the results are presented in Figure 3 (middle panel). $\Delta R_{p_{\Delta\tau}}$ and $\Delta R_{s_{\Delta\tau}}$ are anti-correlated (Pearson correlation coefficient is -0.99, irrespective of the surface albedo), and the magnitude of $\Delta R_{s_{\Delta\tau}}$ increases with an increase in surface albedo. Figure 4 (Middle) shows the partial derivative of the reflectance with respect to τ for increasing surface albedo. ~~The interference between $\Delta R_{p_{\Delta\tau}}$ and $\Delta R_{s_{\Delta\tau}}$~~This anti-correlation explains negative derivatives in the higher surface albedo regime.

$\Delta R_{p_{\Delta\omega}}$ and $\Delta R_{s_{\Delta\omega}}$ of aerosol single scattering albedo (ω) in Figure 3 (right panel) reveals a strong correlation (with a Pearson correlation coefficient of almost unity). This suggests that an increase in surface albedo increases the sensitivity of the model to ω. We suspect that this information predominantly arises from interactions between scattered light by aerosols and surface. The magnitude of the partial derivative of reflectance with respect to ω for increasing surface albedo (shown in Figure 4, bottom) shows an increase, which is in line with our analysis of Figure 3 (right panel).

For increasing surface albedo, the more dynamic parts of the $\partial R/\partial\tau$ spectrum in Figure 4 (Middle) correspond to spectral points with less absorption by molecular oxygen. These are also the parts of the spectrum with a high signal to noise ratio (SNR) and high S_ϵ^{-1}. From Equation 4, the inverse method gives a higher priority to spectral points with a higher S_ϵ^{-1}. Intuitively, low information of τ from the oxygen A-band spectrum will increase the dependency of the inverse method to prior information. This is further discussed in the next section.

3.2 Aerosol-surface interplay in the top of atmosphere reflectance

In the inverse method, an a-priori error of 100% is assumed for the aerosol optical thickness, which gives it freedom to vary during iterations. If the ~~first guess of the~~ a-priori aerosol optical thickness is far from the solution, a large a-priori error ensures that the retrieval can estimate the parameter in fewer iterations. However, whether the Gauss-Newton optimisation reaches the correct solution depends on two primary factors, i. if the cost function has a global minimum, and ii. the the gradient of the cost function is sufficiently large, such that it is minimised significantly at every iteration.

From our analysis of $\Delta R_{\Delta x}$ for aerosol parameters, we have identified aerosol optical thickness to be the parameter most affected by an increasing surface albedo, due to the ~~anti-correlation~~ cancellation between $\Delta R_{p_{\Delta\tau}}$ and $\Delta R_{s_{\Delta\tau}}$ owing to their similar amplitudes, spectral shapes but opposing signs. Because of this, the top-of-atmosphere reflectance spectrum becomes independent of aerosol optical thickness for higher surface albedo regimes (Figure 5).

Over a dark surface such as the ocean, top of atmosphere reflectance in the continuum is unique at different aerosol loads (Figure 5, left panel). The variation in the top of atmosphere reflectance in the continuum reduces as the instrument points more towards the nadir. In such geometries, R_s can play a more significant role than R_p ~~(Figure 2, blue line)~~ and reduce the available information on τ in the $R(\lambda, A_s)$ spectrum. For bright surfaces, the variation in the the top of atmosphere reflectance

spectrum is less for steeper geometries relative to the same geometries over the ocean (Figure 5, middle panel, green and blue line). There can also be cases where, provided sufficiently high aerosol loading, the top of atmosphere reflectance spectrum in the continuum can be independent of aerosol optical thickness over very bright surfaces such as vegetation (Figure 5, right panel, green line). In such cases, more than one values of τ result in the same top of atmosphere reflectance. Henceforth in this paper, this phenomenon is termed as aerosol-surface ambiguity.

A loss in aerosol information can have special implications in the minimisation of the cost function. As observed in Figure 6, for lower surface albedo regimes there exists a single minima of the cost function. For such scenes, if the a-priori aerosol optical thickness is far from the true value, the gradient is sufficiently large such that a small change in the state vector between iterations leads to a significant minimisation of the cost function. As the surface albedo increases, this gradient decreases significantly, and can also result in the presence of multiple minima in the cost function (Figure 6, right) if the state vector is far away from the truth. This makes the retrieval dependent on the initial guess of τ. ~~Also, as R_s increases,~~

Because of a model error (described in Figure 6) in the aerosol layer height between $\mathbf{y}$ and $\mathbf{F}(\mathbf{x}, \mathbf{b})$ (in Equation 2), the global minimum of the cost function shifts away from the true τ. This ~~is predominantly~~ shift is biased higher than the truth if the aerosol layer is lower in the atmosphere in comparison to the aerosol layer in the synthetic true spectrum, because the model has to compensate the extra absorption by molecular oxygen. If the aerosol layer is higher in the atmosphere, the minimum of the cost function is situated at a τ lower than the true τ. As observed in Figure 6 (left, red line)~~over the bright surface~~ , this shift of the cost function minimum from the true τ is larger over bright surfaces for a viewing angle close to nadir, where R_s is more dominant. For the same angle, the global minimum over a dark surface is situated at the true τ value, even with the presence of a model disagreement with the simulated 'true' spectrum. As the viewing angle increases over the bright surface, R_p increases and the global minimum of the cost function moves closer towards the true τ.

If the a-priori error assigned to aerosol optical thickness is large, presence of aerosol-surface ambiguities can result in non-convergences. Because the a-priori part of the cost function has a smaller value than the measurement part, reducing a-priori error assigned to the aerosol optical thickness does not necessarily guarantee a solution to this issue since it does not remove the multiple-minima present in the cost function. Since errors between aerosol optical thickness and aerosol layer height are correlated (Sanders et al., 2015), a large error in the optical thickness will lead to a large error in the aerosol layer height estimate. The next section discusses the sensitivity of the aerosol layer height algorithm to this phenomenon by introducing model errors in a simulation environment.

4 Error analysis

In DISAMAR, forward models for simulation and retrieval have been kept separate so that errors can be introduced into the simulated spectra to mimic errors in a real retrieval scenario. In this section, the instrument model of the Sentinel-4 UVN near infrared spectrometer is used. The wavelength range for simulations and retrievals is between 758 nm and 770 nm. ~~Error analysis is done for the~~ A comparative analysis of biases in the retrieved aerosol layer height ~~retrieval algorithm and a comparison is made between retrievals~~ is conducted over ocean (A_s = 0.03) and land (A_s = 0.25, and A_s = 0.4). Bias in the

aerosol layer height is defined as the difference between ~~true and retrieved~~ retrieved and true aerosol layer height (in hPa) — a ~~negative~~ positive sign indicates that the aerosol layer is retrieved ~~closer to the ground~~below the true aerosol layer height. The aerosol layer height retrieved is a single layer for the entire atmospheric column, with a fixed thickness of 50 hPa.

4.1 Sensitivity to model error in the aerosol layer thickness

In a typical real-world scenario, aerosol plumes can be as thick as 200 hPa in the atmosphere, or more. We simulate a scene containing an aerosol layer that extends approximately from the surface (1000 hPa) to 800 hPa in the atmosphere. The true τ is 1.0, and the a-priori τ is 0.5. The a-priori value of the aerosol layer height is 650 hPa, and the aerosol layer thickness is fixed at 50 hPa. In an ideal retrieval instance, the retrieved aerosol layer height (which has a thickness of 50 hPa) should coincide with the height of the simulated thicker aerosol layer. We observe that, in general, the error in the retrieved aerosol layer height reduces as the viewing zenith angle increases (Figure 7, top left). This is explained by ~~the lowered interference between R_p and~~ a reduction in R_s and an increase in R_p, (Figure 2, red line)~~. This is why the~~ , which explains why difference in errors between retrievals over ~~the~~ different surfaces reduces with an increase in viewing ~~zenith angle~~ angle (Figure 7, top left, high viewing zenith angles).

At lower viewing zenith angles, the difference in aerosol layer height errors between retrievals over the different surfaces is the largest, since the effect of R_s interfering with R_p is significantly larger (Figure 2, blue line), which increases with an increase in surface albedo (Figure 3, left). The retrieved aerosol layer is biased towards the surface in all three surface albedo scenarios, with the aerosol layer being placed closer to the surface if the surface albedo is brighter. ~~While it would appear that somehow the sensitivity of~~ This should not suggest a sensitivity to the geometrical thickness of the aerosol layer. As the surface albedo increases, the ~~retrieval to aerosol layerthickness increases with increasing surface albedo , this behaviour is explained better as perhaps the most interesting consequence of the interference between R_s and R_p ingrained within the optimal estimation framework. To explain its mechanism, the following three inferences are highlighted:~~

~~A look into the Jacobian in Figure 4 (top) shows that , for the same atmospheric conditions and the same aerosol layer height, an increase in surface albedo can reduce the magnitude of $\partial R/\partial z$ (parts of the P-branch between 762 nm and 765 nm, where~~ number of photons that pass through the atmosphere to interact with the surface before reaching the detector increases. These photons have a longer path length, which results in an increased absorption by oxygen ~~is minimal). A reduced magnitude $\partial R/\partial z$ for a spectral point signifies a reduced sensitivity to aerosol layer height at that spectral point. Figure 3 (left) shows low interference between $\Delta R_{p_{\Delta z}}$ and $\Delta R_{s_{\Delta z}}$ at spectral points with high absorption by oxygen , and vice versa. This suggests that, while parts of the spectrum with high absorption remain more-or-less the same irrespective of an increase in surface albedo, the parts with lower absorption get altered. From Figure 1 (right), it is observed that aerosol layers situated lower in the atmosphere have relatively deeper absorption lines~~at ~~spectral sub-bands with low absorption by oxygen . Assuming shot noise, parts of the spectrum with a lower absorption by oxygen~~ specific spectral points with weak oxygen absorption lines. In comparison to photons at wavelengths with strong oxygen absorption lines, these photons have a higher SNR since relatively more of them reach the detector. A higher SNR ensures lower noise, and hence a higher value in the inverse of the measurement error covariance matrix S_ϵ. If a spectral point has a higher value in S_ϵ^{-1} ~~than parts of the spectrum with a higher absorption by~~

~~oxygen. From Equation 4, a higher weight is given to these points in deciding the update to the state vector and in the overall optimal estimation framework.~~

~~Because of the interference between R_p~~ matrix, it has a higher representation in the cost function (in Equation 2), and ~~R_s, parts of the oxygen A-band spectrum with high SNR (and~~ hence a higher ~~weight~~ preference (or weight) in the optimal estimation~~) appear to have more absorption for observations over high surface albedos, corresponding to~~. Because of this, the retrieval prefers to retrieve an aerosol layer height described by photons that travel through the aerosol layer closer to the surface~~than the true aerosol layer height.~~. If, however, the aerosol optical thickness is so large that the photons cannot penetrate the aerosol layer, the retrieved aerosol layer height would be more accurate. Retrieving height of optically thin aerosol layers can also be quite challenging, owing to the fact that these layers will allow more photons to pass through and interact with the surface, leading to an increase in R_s, and hence an increase in the cancellation between R_p and R_s. As a result of this, large biases in the retrieved aerosol layer height can be expected for optically thin layers over bright surfaces.

Another consequence of retrieving aerosol layer height ~~in the presence of interference between R_s and R_p~~ over bright surfaces is that the retrieval may become more susceptible to model error in aerosol and surface properties, such as the aerosol phase function anisotropy factor g, the aerosol single scattering albedo ω and especially the surface albedo A_s, which are fixed in the model. These are investigated in the following.

4.2 Sensitivity to model error in the aerosol phase function

The presence of a model error in the aerosol phase function can result in large biases if the surface is bright (Figure 7, top right). For a higher surface brightness and a viewing angle close to nadir, this bias is larger. As the viewing angle increases, the biases reduce significantly. The correlation of bias with surface albedo suggests that ~~a~~ biases cause by model errors are exacerbated by the surface contribution R_s, which reduces as viewing angle increases (Figure 2, right).

4.3 Sensitivity to model error in aerosol single scattering albedo

From Figure 4, aerosol single scattering albedo plays an increasingly significant role in the retrieval of aerosol layer height as the surface gets brighter. Because of this, a mis-characterisation of aerosol single scattering albedo in the model can lead to very large biases over bright surfaces (Figure 7, bottom left), and also non-convergences. This is not the case for retrievals over the ocean, since the influence of aerosol single scattering albedo on the oxygen A-band spectrum is low. It is observed that, as the viewing angle increases, these biases drop significantly. This is again attributed to the ~~decreased interference between R_p and~~ decrease in R_s and increase in R_p with increasing viewing angle (again, over a Lambertian surface).

4.4 Sensitivity to model error in surface albedo

Surface albedo is a critical component in the accurate retrieval of aerosol layer height over bright surfaces. Because it is a fixed parameter in the forward model, an error in the surface albedo can result in large biases in the retrieval. To simulate model errors, relative errors of -10% to 10% are introduced in the retrieval forward model, such that the surface is modeled darker

or brighter than the true value. For relative errors of $\pm 10\%$, the retrieved aerosol layer height can be biased more than two orders of magnitude larger over land than ~~the over the~~ over ocean (Figure 7, bottom right). For retrievals over a bright surface such as vegetation (A_s = 0.4 or greater), the model error can result in non-convergences. As the model error reduces, retrievals over land with a surface albedo of 0.25 become more acceptable. However, over very bright surfaces, an inaccuracy in surface albedo of more than 2% can result in biases greater than 100 hPa.

~~The sign of aerosol layer height retrieval biases is dependent on the sign of the error in the surface albedo. If the a-priori surface albedo is greater than the true surface albedo, the aerosol layer height is estimated much closer to the ground. From our analysis of splitting the oxygen A-band spectrum into R_p and R_s, we understand that this has to do with the increased R_s due to the surface albedo fixed at a higher value.~~

The next section demonstrates the implication of these errors in a real retrieval scenario.

5 Demonstration case: 2010 Russian wildfires

The 2010 Russian wildfires began in late July and lasted for several weeks until the beginning of September. Literature reports droughts and record summer temperatures in the same year as a precursor to the wildfires, both of which have been attributed to climate change (Hansen et al., 2012). A consequence of the forest fires were optically thick aerosol plumes over the country, especially over Moscow. In the first few weeks of August, 2010, due to the presence of a strong anti-cyclonic circulation pattern in the atmosphere, the impact of biomass burning aerosols on air quality in Moscow was markedly larger than what was observed from previous wildfire incidences — the UV Aerosol Index (AI) reported by the Ozone Monitoring Instrument (OMI) on board the NASA Aura mission observed an increase by a factor of 4.1 from previous years (Witte et al., 2011) over Moscow, due to aerosol plumes originating from the South and East of the city.

The aerosol plume above Russia on the 8th of August, 2010 serves as a test case for the aerosol layer height retrieval algorithm, due to fairly cloud-free conditions and the optical thickness of the aerosol plume (see Figure 8, right). Because of this, we do not employ a cloud-screening method. The GOME-2A instrument crosses over the scene at approximately 09:45 hrs - 09:47 hrs at local time. The GOME-2A pixels within the region of interest are recorded between 0745 hrs UTC and 0748 hrs UTC, at approximate latitude bounds of 52° and 60° and longitude bounds 29° and 45°. This corresponds to 255 pixels in total. Meteorological information relevant to the retrieval are temperature-pressure profiles and surface pressure, acquired from the European Center for Medium-Range Weather Forecast (ECMWF) ERA-Interim database (Dee et al., 2011) at the GOME-2A pixel using nearest neighbour interpolation. Surface albedo is derived using nearest neighbour interpolation for version 1.3 of GOME-2A LER climatology derived from Tilstra et al. (2017), ~~who provide monthly Lambertian Equivalent Reflectivity (LER) climatologies on a 0.5~~which is at a 1° x ~~0.5~~1° grid. Typical values of the surface albedo over the region of interest is around 0.21. In the inverse method, the ~~first guess~~ a-priori value of the aerosol layer height is approximately 800 hPa. The a-priori aerosol optical thickness is 1.0 at 760 nm.

CALIOP data is used for validation, which provides vertical distribution of aerosols and clouds for a footprint of approximately 70 m, with a 5 km horizontal resolution (Winker et al., 2009). While the coverage of the instrument is not as expansive

as the GOME-2 instrument, the level of information available from CALIOP gives a good idea on the vertical position of aerosols in the atmosphere. For a better validation dataset, CALIOP data recorded between coordinates 52.0° latitude and 64.0° latitude, approximately around 1045 hrs UTC is used for comparison of GOME-2A aerosol layer height retrieval results. The Level-1 CALIOP attenuated backscatter data from 1064 nm is used because lidar in the visible region (532 nm) can get heavily attenuated over optically thick plumes. As can be seen from Figure 9, the aerosol layer is situated in between the surface and 5 km above the surface. In total, 82 GOME-2A pixels falling within 100 km of the CALIPSO track are considered for comparison.

The operational algorithm retrieves aerosol layer height and aerosol optical thickness, with fixed a-priori values, as mentioned in Table 1. Following evaluation of the algorithm on GOME-2A pixels by Sanders et al. (2015), the surface albedo is not included in the state vector. The single scattering albedo is not fitted in the sensitivity analyses in order to maintain consistency with the current operational algorithms for the Sentinel missions, which currently do not fit this parameter.

Table 1. A-priori and validation information required to process data over 2010 Russian wildfires on the 8^{th} of August, 2010.

parameter	**source**	**remarks**
radiance and irradiance	GOME-2A	data between latitudes 52° and 60° and longitudes 29° and 45° (255 pixels)
solar and satellite geometry	GOME-2A Level 1-b data	
surface albedo A_s	Tilstra et al. (2017)	~~GOME-2 LER at 0.5~~GOME-2A LER at 1° x ~~0.5~~1° grid at 758 nm and 772 nm
surface pressure p_s	ERA-Interim	
temperature pressure profile	ERA-Interim	
aerosol optical thickness τ		state vector element, a-priori = 1.0
aerosol layer height h_{mid} [km]		state vector element, a-priori = p_s - 200 hPa
aerosol single scattering albedo ω		fixed at 0.95
aerosol phase function $P(\theta)$		Henyey-Greenstein with asymmetry factor g of 0.7
cloud mask		none
validation	CALIOP lidar profiles	5 km × 5 km total attenuated backscatter at 1064 nm

5.1 Results from the retrieval algorithm

Out of the chosen 255 GOME-2A pixels, 155 pixels converged and 100 pixels failed to converge to a solution (40% of the pixels do not converge). The algorithm retrieved aerosol layers primarily in the lower troposphere, roughly within 0 - 3 kilometers (Figure 8, left). The mean aerosol layer height retrieved is 714 m above the ground with a standard deviation of 647 m and a median of 450 m. The retrieved aerosol layers are optically thick (Figure 8, middle), with an mean retrieved aerosol optical

thickness of 3.0, a standard deviation of 1.8, and a median of 2.5. The retrievals over the primary aerosol plume do not converge to a solution.

Figure 9 (top) provides results of retrieving aerosol layer height over the chosen 82 GOME-2A pixels ~~colocated~~ co-located to the CALIPSO track. The CALIOP backscatter data shows that the aerosol plume extends from the ground to approximately 4 km between latitudes 53° and 60°. Beyond 60° latitude, the aerosol layer is elevated. Of the 82 pixels, 52 converge to a solution. From Figure 9, it is observed that the retrieved aerosol layer heights are generally biased closer to the surface. ~~From our analysis in Figure 7 (top left), we understand this to be a consequence of the interference between R_p and R_s in the presence of model error in the aerosol layer thickness~~This is explained by the increase in surface contribution R_s which represents photons passing through the atmosphere and interacting with the surface before reaching the detector. The spectral points representing these photons have a higher weight in the optimal estimation in comparison to the photons that do not interact with the surface and hence the aerosol layer height is retrieved closer to the surface.

In Figure 9, the retrieval does not converge to a solution between latitudes 57° and 60°. This area also corresponds to the primary biomass burning plume in Figure 8. However, the estimated aerosol layer height in the last iteration for these pixels seems to be located within the aerosol plume (Figure 9, top, white crosses between latitudes 57° and 60°). To investigate this, we retrieve τ from the top-of-atmosphere reflectance in the continuum with different a-priori optical thickness values in order to test whether the non-uniqueness of aerosol optical thickness is a potential cause of retrieval non-convergence.

5.2 Retrieving aerosol layer height with multiple a-priori aerosol optical thickness values

Aerosol optical thickness (τ) is first retrieved from the continuum before the oxygen A-band between 755 nm - 756 nm. τ is retrieved with two a-priori values τ_a and τ_b. In these retrievals, the aerosol layer height is kept fixed at any arbitrary value, since its value will hardly affect the continuum.

First, τ_a = 1.0 is chosen, and the retrieved solution $\tau_a^{'}$ is then used to decide the a-priori value τ_b. If the solution for $\tau_a^{'}$ is not reached, then $\tau_b^{'}$ is not calculated. In the case that $\tau_a^{'}$ is retrieved, τ_b is chosen in the following manner,

$$\tau_b = \begin{cases} \tau_a^{'}/2 & \text{if } \tau_a^{'} < \tau_a \\ \tau_a^{'} + 0.5 & \text{if } \tau_a \leq \tau_a^{'} < 10.0. \end{cases} \tag{8}$$

If the retrieval for $\tau_b^{'}$ fails, then we can infer a dependence on a-priori information. If the retrieval is successful, $\tau_a^{'}$ and $\tau_b^{'}$ are compared to check if they are similar using the following criterion,

$$\tau_a^{'} \approx \tau_b^{'} \text{ if } \mathbf{abs}(\tau_a^{'} - \tau_b^{'}) < T \times \mathbf{min}(\tau_a^{'}, \tau_b^{'}), \tag{9}$$

where T is a threshold, chosen to be 0.15. Increasing this threshold increases the margin of similarity of $\tau_a^{'}$ and $\tau_b^{'}$. This method is henceforth called the prefit method.

Applying the prefit method to the GOME-2A pixels processed previously, it is observed that out of 255 pixels, 215 pixels retrieve $\tau_a^{'}$ and 40 pixels do not. Upon analysis of these 40 pixels, it is observed that the these pixels do not converge because the retrieved aerosol optical thicknesses are in excess of 10.0, and DISAMAR stops the retrieval since τ reaches boundary conditions (beyond 20.0). Such large optical thicknesses may be attributed to the saturation of the top of atmosphere reflectance at very high aerosol loads, observed in Figure 5. It is also possible that these retrievals do not converge because of the presence of other model errors. Two pixels retrieve $\tau_a^{'}$ above 10.0, and hence are not considered for retrieving $\tau_b^{'}$.

From these 213 pixels, 209 pixels converge to $\tau_b^{'}$, whereas four pixels do not converge to a solution. These four pixels that do not converge are confirmed cases of the presence of aerosol-surface ambiguities, since the retrieval toggles between two values at every iteration until the maximum number of allowable iterations is reached. This is also a consequence of a non-unique top of atmosphere reflectance at high aerosol load scenarios. Out of the 209 pixels that retrieve both $\tau_a^{'}$ and $\tau_b^{'}$, 205 pixels have similar retrieved optical thickness values according to criterion in Equation 5.2. The rest have values which are off by more than 2.0.

From Figure 8 (right), pixels that contain aerosol-surface ambiguities primarily lie within the main aerosol plume. This is in-line with our expectation of the top of atmosphere being saturated at very high aerosol loads. Interestingly, these pixels also comprise 50% of the pixels that do not converge for aerosol layer height retrieval. Figure 9 (bottom) provides a plot of the retrieval of CALIPSO co-located GOME-2A pixels, in which 22 pixels are absent from the plot (relative to Figure 9, top). These are pixels for which the prefit method retrieves different $\tau_a^{'}$ and $\tau_b^{'}$.

5.3 Discussion

Out of the 100 pixels that do not converge, 50 pixels have been identified which may be affected by aerosol-surface ambiguities. For a majority of these pixels, the retrieved aerosol optical thickness is typically beyond 4.0~~, for which we can expect multiple minima in the cost function~~. It is possible that the true number of pixels that are affected by aerosol-surface ambiguities are higher than 50 pixels — our analysis is represented by a similarity criterion which relies on a similarity threshold T, which we have set at 15% (Equation 5.2). With a more strict criterion, more pixels affected by aerosol-surface ambiguities may be detected. Other non-convergences may be a result of model errors. Comparing our retrievals with the CALIOP attenuated backscatter profile from the infrared channel, we observe that our retrievals are biased closer to the surface, with non-convergences occurring for pixels within the primary biomass burning plume.

6 Conclusions

~~There exists an interference between scattered light by aerosols and the surface to the top of atmosphere reflectance in~~ Depending on the surface brightness, the interaction of photons scattered from the atmosphere and the surface can result in a possible reduction of available aerosol information in the oxygen A-band spectrum. Our basis for this assertion depends on the distinction of aerosol information present in atmospheric path contributions R_p and surface contributions R_s to the top of atmosphere reflectance in the spectrum (Figure 2). ~~These interferences are dominant in high surface albedo regimes~~

and viewing geometries close to the nadir. A consequence of this interference is a reduction in the amount of information the oxygen A-band spectra has on aerosol parameters. The reduction of aerosol information increases with increasing surface brightness and decreasing viewing angle.

Our analyses reveal that the information available on aerosol optical thickness in derivatives of the atmospheric path and surface contribution contributions with respect to aerosol optical thickness are anti-correlated (see Figure 3, middle), which affects the derivative of reflectance with respect to aerosol optical thickness changes (see Figure 4). As the surface gets brighter, the magnitude of this derivative decreases, which reduces the sensitivity of the oxygen A-band spectrum to aerosol optical thickness. We expect this anti-correlation behaviour to be strong for viewing angles closer to the nadir, since the interference between R_p increases and R_s reduces decreases with an increase in viewing angle (see Figure 2). One of the consequences of this interference is the effect on cost function for retrieving aerosol optical thickness. We report that the gradient of the cost function tends to become more shallow as the surface albedo increases. This is especially the case when the viewing angle is closer to the nadir (see Figure 6). We also notice the that the cost function reduces at high aerosol optical thickness beyond the local minimum near the truth (Figure 6, right), which indicates the presence of multiple minima in the cost functionfor high aerosol optical thickness values. We attribute this behaviour to the saturation of the top of atmosphere reflectance at high aerosol loads (see Figure 5).

Similar analyses on the available information on aerosol layer height in R_p and R_s in the oxygen A-band reveals that parts of the oxygen A-band spectrum with a low absorption by oxygen have interference between R_p and R_s an increased cancellation of $\Delta R_{p\Delta z}$ and $\Delta R_{s\Delta z}$ (see Figure 3, left) , which are primarily prevalent over bright surfaces (such as land). and hence a reduction in aerosol layer height sensitivity in specific parts of the spectrum (see Figure 7, top). This increases as surface albedo increases. It is also observed that the information content available on aerosol single scattering albedo (ω) in R_p and R_s are positively correlated derivative of $\Delta R_{p\Delta\omega}$ and $\Delta R_{s\Delta\omega}$ are both positive (see Figure 3, right), which increases the overall sensitivity of the oxygen A-band spectrum to ω with increasing surface albedo. This is observed in the derivative of reflectance with respect to ω, which increases in magnitude with an increase in surface albedo.

This interference of The interaction between photons scattering back from the atmosphere ($R_p$and) to the detector and photons that travel through the atmosphere to the surface and back to the detector (R_s) has direct consequences to the retrieval of aerosol layer height from the oxygen A-band. Over bright surfaces, the retrieval algorithm becomes increasingly susceptible to errors in the aerosol layer height estimates as well as non-convergences in the presence of model errors (see Figure 7). The interference of R_p and R_s sign difference of $\Delta R_{p\Delta z}$ and $\Delta R_{s\Delta z}$ also explains why retrieving a aerosol layer over bright surfaces with a 50 hPa thickness for thicker layer (say 200 hPa thickness) can be biased closer to the ground (see Figure 7, top left). To demonstrate this assertion in a real retrieval scenario, we have retrieved aerosol layer height over the 2010 Russian wildfires in the 8th of August, 2010, using measured oxygen A-band spectra recorded by the GOME-2 instrument on board the Metop-A satellite. For validating our retrievals, we refer to lidar measurements by the CALIOP instrument on board the CALIPSO mission which records, among other measurements, attenuated backscatter at 1064 nm over the same wildfires scene a few hours after the GOME-2A acquisition. Comparison of co-located GOME-2A and CALIPSO pixels reveals that, in the case of both boundary and elevated aerosol layers, the retrieved aerosol layer height is biased closer to the surface. For

pixels with a high aerosol load, the algorithm fails to converge to a solution (see Figure 8). Over optically thick plumes, the retrieval becomes dependent on the a-priori aerosol optical thickness (see Figure 8, right). This is, again, a consequence of the interference between R_p and R_s.

Following the work presented in this paper, our further goal is to apply the knowledge gained from this study in the development of the aerosol layer height retrieval algorithm for retrieving aerosols over land.

Acknowledgements. This research is partly funded by the European Space Agency (ESA) within the EU Copernicus programme under the project name 'Sentinel-4 Level-2 Processor Component Development', number AO/1-7845/14/NL/MP. We acknowledge EUMETSAT for providing the GOME-2 L1b data.

Competing interests. The author declares no conflict of interests in the work expressed in this publication.

Figures

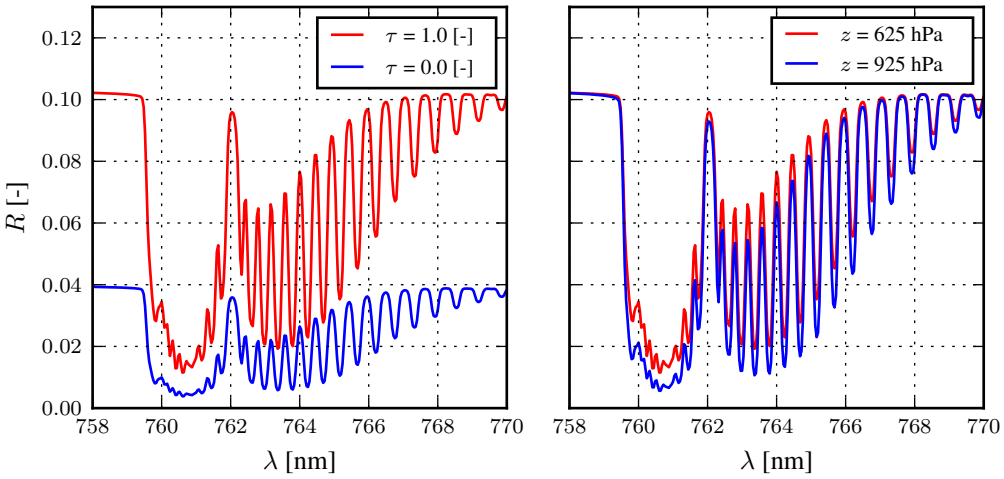

Figure 1. Synthetic oxygen A-band spectra for a cloudless atmosphere containing aerosols over a surface with an albedo of 0.03, as measured by a nadir pointing instrument for a solar zenith angle at 45°. The instrument settings are that of the UVN instrument. Aerosol single scattering albedo is fixed at 0.95 and scattering by aerosols is described by a Henyey-Greenstein phase function with an asymmetry factor (g) of 0.7. **Left**: Aerosol layer is fixed at a height of 900 hPa - 950 hPa, for two scenes are different aerosol optical thicknesses. **Right**: Aerosol vertical distribution is varied for an aerosol optical thickness of 1.0 at 760 nm.

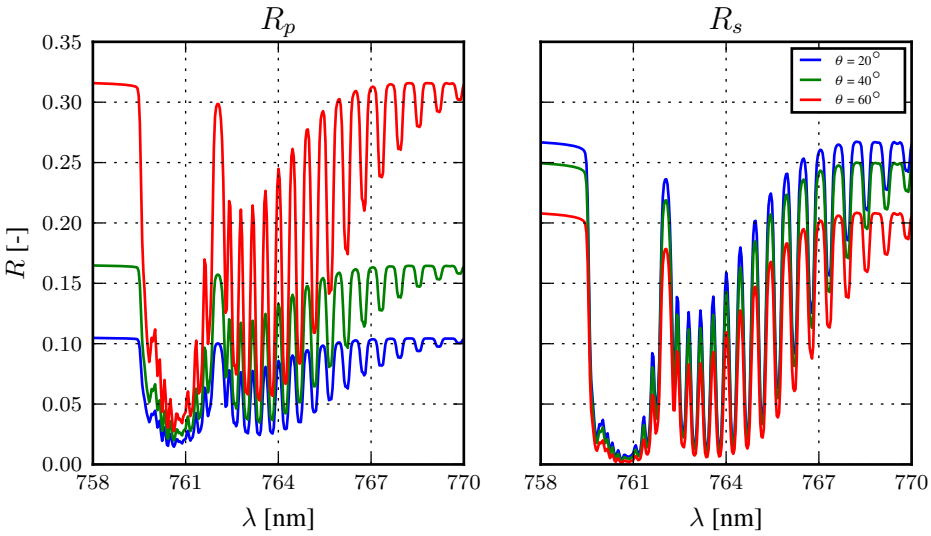

Figure 2. R_p and R_s for increasing viewing zenith angle θ over a surface with an albedo of 0.4 at 760 nm. The solar zenith angle is fixed at 45° and a relative azimuth angle of 0°. Aerosol optical thickness is fixed at 1.0 for an aerosol single scattering albedo of 0.95. Aerosol scattering phase function is a Henyey-Greenstein with g = 0.7. The aerosol layer is situated at 600 hPa, with a thickness of 50 hPa.

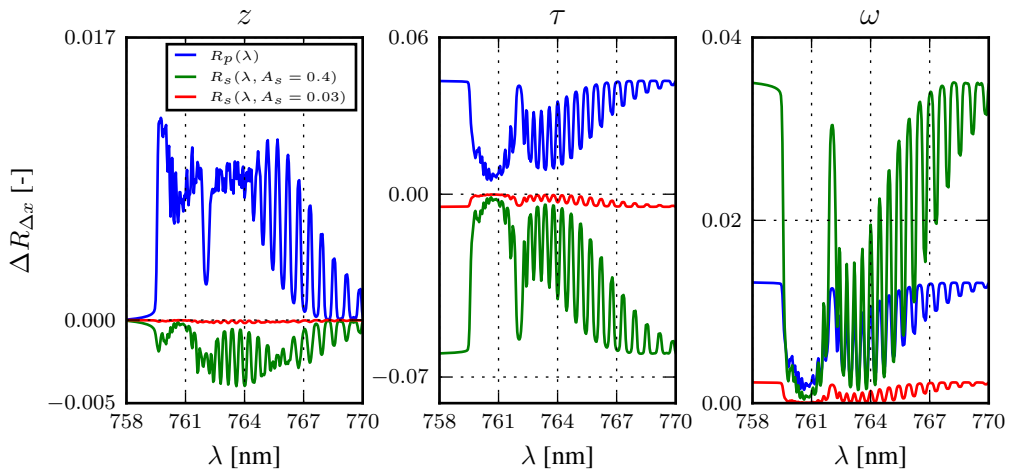

Figure 3. $\Delta R_{p_{\Delta x}}$ (in blue) and $\Delta R_{s_{\Delta x}}$ (in red for A_s = 0.03 and green for A_s = 0.4) to model parameter x in the oxygen A-band, as measured by a nadir pointing instrument for a solar zenith angle at 45°. $\Delta R_{p_{\Delta x}}$ is calculated as the difference of the modeled top-of-atmosphere reflectance between two atmospheres, both cloudless and contain aerosols, which differ only in the parameter x for values x_a and x_b, according to Equation 6. The phase function is described by a Henyey-Greenstein model with an anisotropy factor of 0.7, and the thickness of the aerosol layer is fixed at 50 hPa. **Left**: τ = 1.0 and ω = 0.95 with different aerosol layer heights, z_a = 600 hPa and z_b = 800 hPa. **Middle**: τ_a = 1.0 and τ_b = 0.5 at z = 600 hPa and ω = 0.95. **Right**: τ = 1.0 and z = 600 hPa for ω_a = 0.95 and ω_b = 0.9. Y-axis has optimised per plot.

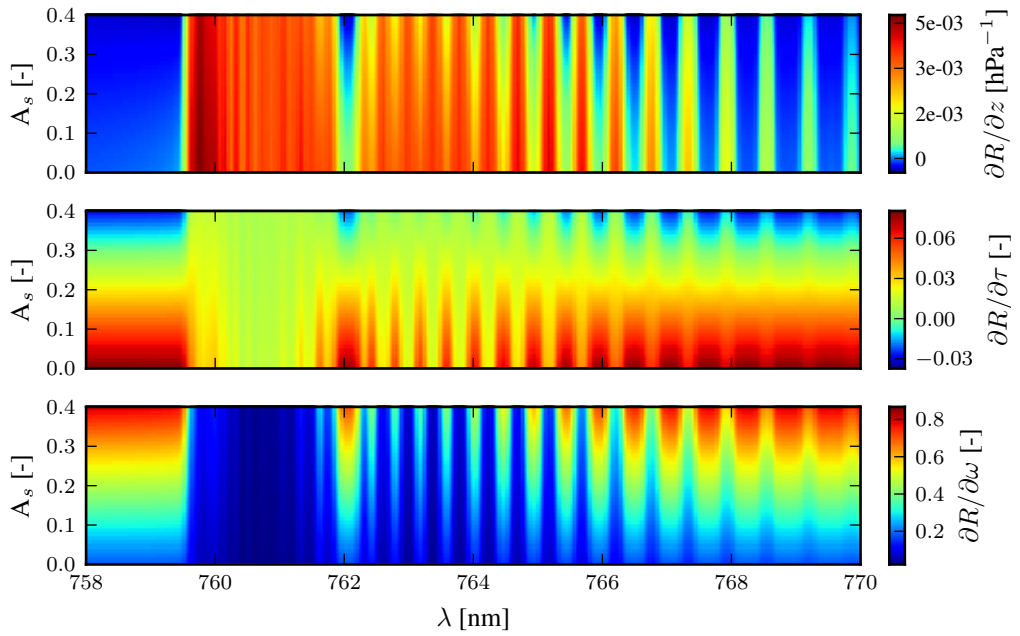

Figure 4. Derivative of reflectance with respect to aerosol properties for different surface albedos A_s. The z is centered around 600 hPa, with τ = 1.0, ω = 0.95, and a Henyey-Greenstein phase function with g = 0.7. The solar zenith angle is 45° and the viewing zenith angle is 0°. **Top**: derivative of reflectance with respect to z. **Middle**: derivative of reflectance with respect to τ. **Bottom**: derivative of reflectance with respect to ω. The colorbar has optimised per plot.

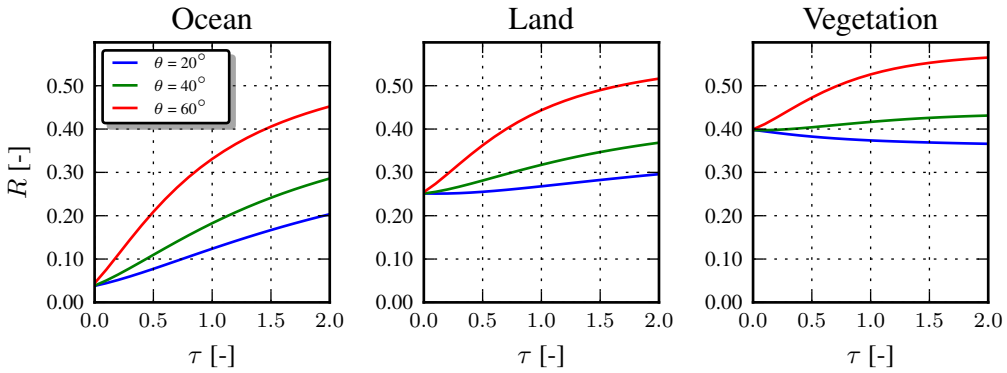

Figure 5. Top-of-atmosphere reflectance at 755 nm, well outside the oxygen A-band, from simulated spectra of scenes containing aerosols over dark and bright surfaces. Red, blue and green lines represent different viewing zenith angles θ, as a function of increasing aerosol optical thickness. Aerosols have a single scattering albedo of 0.95, and the aerosol scattering is described by a Henyey-Greenstein phase function with $g = 0.7$. Aerosol layer is situated at 925 hPa. The solar zenith angle is 45° and a relative azimuth angle is 0°. **Left**: The surface albedo is 0.03 at 760 nm, typical over the ocean. **Middle**: The surface albedo is 0.25 at 760 nm, typical over land. **Right**: The surface albedo is 0.4 at 760 nm, typical over vegetated land.

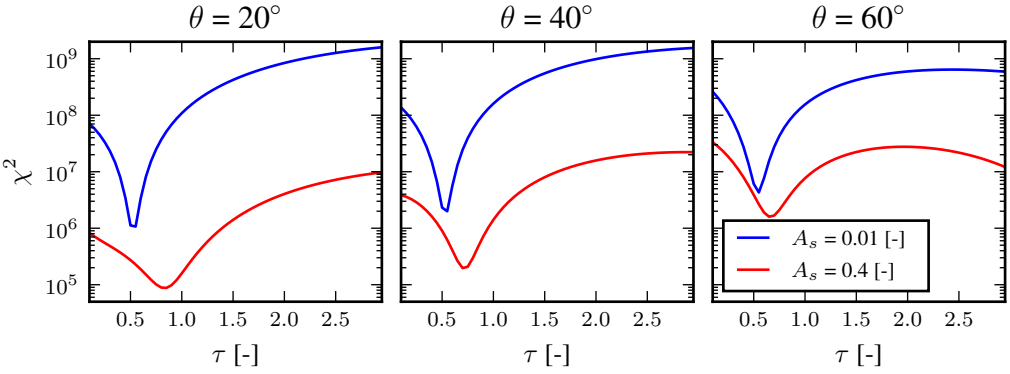

Figure 6. Cost function (χ^2) for retrieving aerosol optical thickness as a function of aerosol optical thickness per iteration (τ) for a dark and a bright surface. The true aerosol optical thickness is 0.5, and the aerosol layer is situated at 600 hPa with a 50 hPa layer thickness. The aerosol single scattering albedo is fixed at 0.95, for a Henyey-Greenstein aerosol phase function with $g = 0.7$. The solar zenith angle is fixed at 45° for varying viewing angles as specified in the plot titles. The relative azimuth angle is 0°. The state vector also contains aerosol layer height, whose a-priori value is fixed at 700 hPa.

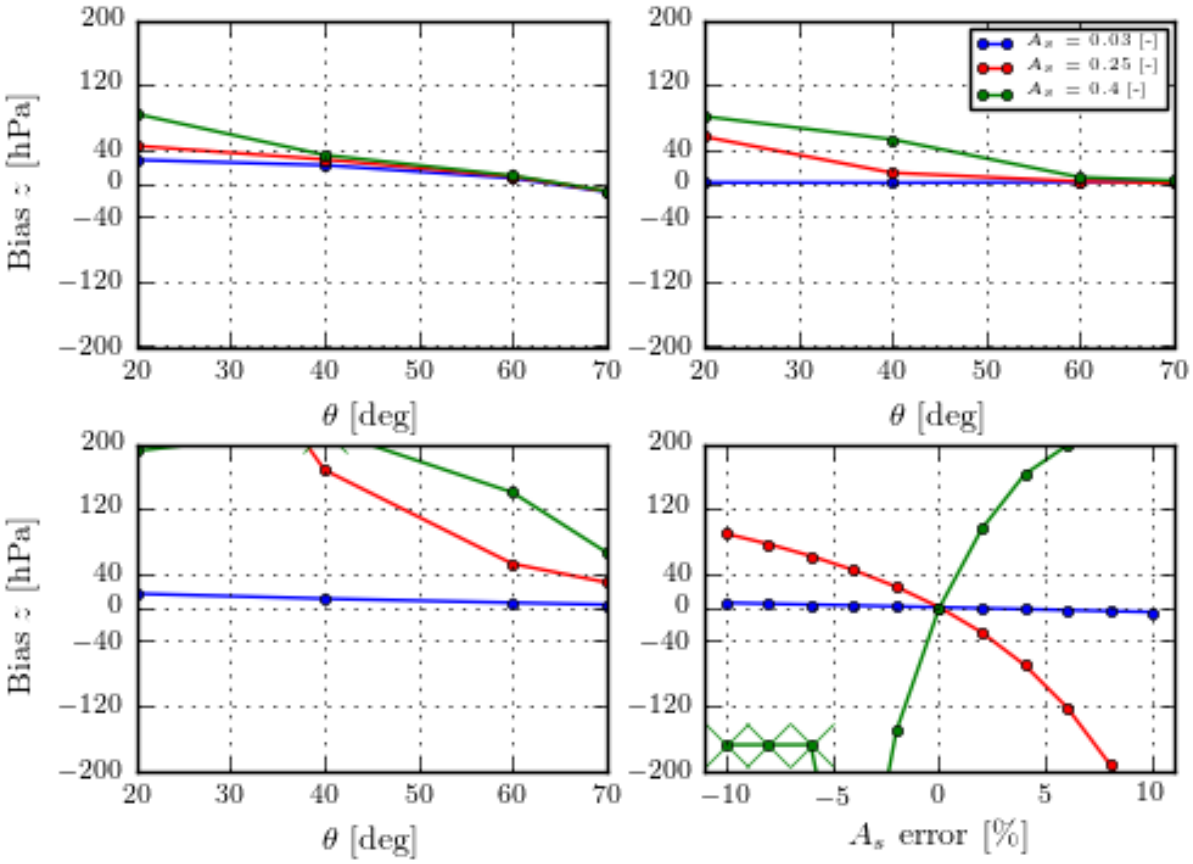

Figure 7. Bias in aerosol layer height in the presence of model errors. Unless specified, the relative azimuth angle is 0° and the solar zenith angle is 45°, aerosol single scattering albedo of 0.95 and Henyey-Greenstein g of 0.7, and an aerosol layer at 650 hPa. **Top left**: Model error is introduced in the thickness of the aerosol layer. The simulated spectra contains a 200 hPa thick aerosol plume extending from the 1000 hPa to 800 hPa. **Top right**: Model error is introduced in the aerosol phase function. The simulated scenes contain aerosols with scattering physics described by a Henyey-Greenstein phase function with g = 0.65 and retrieved with g = 0.7. **Bottom left**: Model error is introduced in the single scattering albedo. The simulated spectra contains aerosols with ω = 0.95, which is fixed in the retrieval forward model at 0.90. **Bottom right**: A relative error is introduced in the surface albedo. The viewing angle is fixed at 20°.

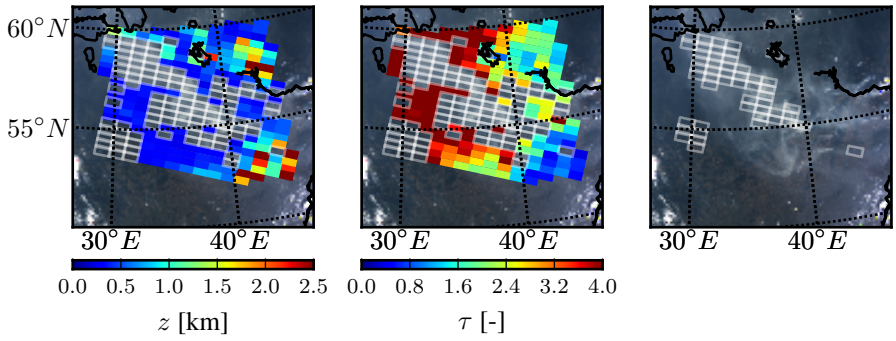

Figure 8. Left: Retrieved aerosol layer height from GOME-2A measurements of the 2010 Russian wildfires, in kilometers above the ground with the aerosol layer height retrieval algorithm. Empty white boxes represent pixels that do not converge to a solution. **Middle**: Retrieved aerosol optical thickness from the same retrievals. **Right**: GOME-2A pixels for which there exist possible aerosol-surface ambiguities (empty pixels with white borders).

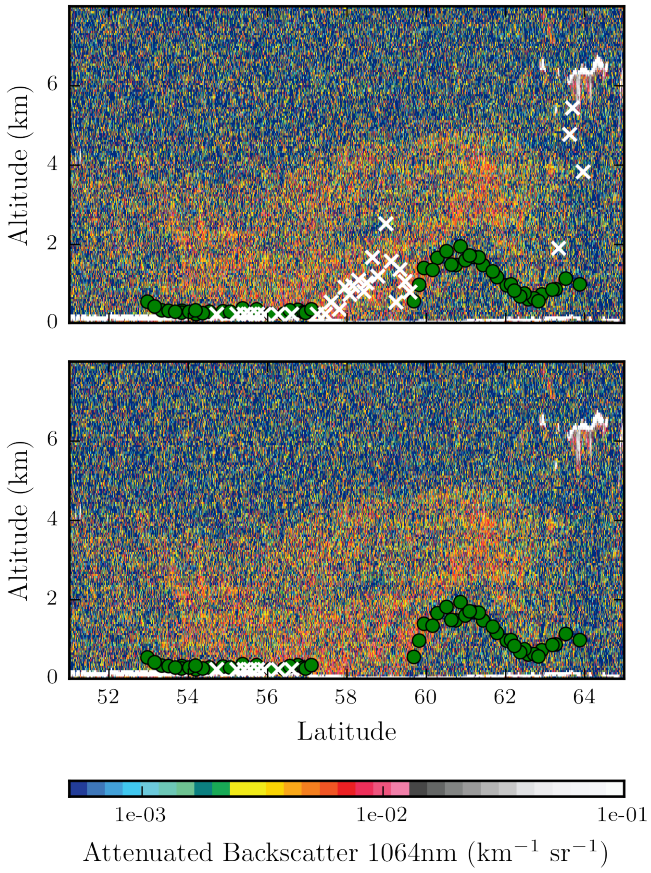

Figure 9. CALIOP lidar backscatter cross-section of a track falling within the region of interest over the 2010 Russian wildfire plume on 8th of August, 2010. **Top**: green dots and white crosses are GOME-2A pixels falling within 100 km of the CALIPSO ground track — green dots represent converged aerosol layer heights, and white crosses represent the aerosol layer heights at the last iteration for pixels that do not converge to a solution. These retrieved altitudes are reported in km above ground surface. **Bottom**: Retrieval results are presented for pixels for which the the prefit method retrieves both $\tau_a^{'}$ and $\tau_b^{'}$ at similar values.

References

Chance, K. and Kurucz, R.: An improved high-resolution solar reference spectrum for earth's atmosphere measurements in the ultraviolet, visible, and near infrared, Journal of Quantitative Spectroscopy and Radiative Transfer, 111, 1289–1295, https://doi.org/10.1016/j.jqsrt.2010.01.036, http://linkinghub.elsevier.com/retrieve/pii/S0022407310000610, 2010.

Chung, C. E. and Zhang, G. J.: Impact of absorbing aerosol on precipitation: Dynamic aspects in association with convective available potential energy and convective parameterization closure and dependence on aerosol heating profile: IMPACT OF AEROSOL ON PRECIPITATION, Journal of Geophysical Research: Atmospheres, 109, n/a–n/a, https://doi.org/10.1029/2004JD004726, http://doi.wiley.com/10.1029/2004JD004726, 2004.

Corradini, S. and Cervino, M.: Aerosol extinction coefficient profile retrieval in the oxygen A-band considering multiple scattering atmosphere. Test case: SCIAMACHY nadir simulated measurements, Journal of Quantitative Spectroscopy and Radiative Transfer, 97, 354–380, https://doi.org/10.1016/j.jqsrt.2005.05.061, http://www.sciencedirect.com/science/article/pii/S0022407305002207, 2006.

de Haan, J. F., Bosma, P. B., and Hovenier, J. W.: The adding method for multiple scattering calculations of polarized light, Astronomy and Astrophysics, 183, 1987.

Dee, D. P., Uppala, S. M., Simmons, A. J., Berrisford, P., Poli, P., Kobayashi, S., Andrae, U., Balmaseda, M. A., Balsamo, G., Bauer, P., Bechtold, P., Beljaars, A. C. M., van de Berg, L., Bidlot, J., Bormann, N., Delsol, C., Dragani, R., Fuentes, M., Geer, A. J., Haimberger, L., Healy, S. B., Hersbach, H., Hólm, E. V., Isaksen, L., Kållberg, P., Köhler, M., Matricardi, M., McNally, A. P., Monge-Sanz, B. M., Morcrette, J.-J., Park, B.-K., Peubey, C., de Rosnay, P., Tavolato, C., Thépaut, J.-N., and Vitart, F.: The ERA-Interim reanalysis: configuration and performance of the data assimilation system, Quarterly Journal of the Royal Meteorological Society, 137, 553–597, https://doi.org/10.1002/qj.828, http://doi.wiley.com/10.1002/qj.828, 2011.

Hansen, J., Sato, M., and Ruedy, R.: Perception of climate change, Proceedings of the National Academy of Sciences, 109, E2415–E2423, https://doi.org/10.1073/pnas.1205276109, http://www.pnas.org/cgi/doi/10.1073/pnas.1205276109, 2012.

Henyey, L. C. and Greenstein, J. L.: Diffuse radiation in the Galaxy, The Astrophysical Journal, 93, 70, https://doi.org/10.1086/144246, http://adsabs.harvard.edu/doi/10.1086/144246, 1941.

Ingmann, P., Veihelmann, B., Langen, J., Lamarre, D., Stark, H., and Courrèges-Lacoste, G. B.: Requirements for the GMES Atmosphere Service and ESA's implementation concept: Sentinels-4/-5 and -5p, Remote Sensing of Environment, 120, 58–69, https://doi.org/10.1016/j.rse.2012.01.023, http://linkinghub.elsevier.com/retrieve/pii/S0034425712000673, 2012.

IPCC: Clouds and Aerosols, in: Climate Change 2013 - The Physical Science Basis, pp. 571–658, Cambridge University Press, Cambridge, http://ebooks.cambridge.org/ref/id/CBO9781107415324A024, dOI: 10.1017/CBO9781107415324.016, 2014.

Landgraf, J., Hasekamp, O. P., Box, M. A., and Trautmann, T.: A linearized radiative transfer model for ozone profile retrieval using the analytical forward-adjoint perturbation theory approach, Journal of Geophysical Research: Atmospheres, 106, 27 291–27 305, https://doi.org/10.1029/2001JD000636, http://doi.wiley.com/10.1029/2001JD000636, 2001.

Munro, R., Lang, R., Klaes, D., Poli, G., Retscher, C., Lindstrot, R., Huckle, R., Lacan, A., Grzegorski, M., Holdak, A., Kokhanovsky, A., Livschitz, J., and Eisinger, M.: The GOME-2 instrument on the Metop series of satellites: instrument design, calibration, and level 1 data processing – an overview, Atmospheric Measurement Techniques, 9, 1279–1301, https://doi.org/10.5194/amt-9-1279-2016, http://www.atmos-meas-tech.net/9/1279/2016/, 2016.

Rodgers, C. D.: Inverse methods for atmospheric sounding: theory and practice, vol. 2, World Scientific, 2000.

Sanders, A. F. J. and de Haan, J. F.: Retrieval of aerosol parameters from the oxygen A band in the presence of chlorophyll fluorescence, Atmospheric Measurement Techniques, 6, 2725–2740, https://doi.org/10.5194/amt-6-2725-2013, http://www.atmos-meas-tech.net/6/2725/2013/, 2013.

Sanders, A. F. J. and de Haan, J. F.: TROPOMI ATBD of the Aerosol Layer Height product, http://www.tropomi.eu/sites/default/files/files/S5P-KNMI-L2-0006-RP-TROPOMI_ATBD_Aerosol_Height-v1p0p0-20160129.pdf, 2016.

Sanders, A. F. J., de Haan, J. F., Sneep, M., Apituley, A., Stammes, P., Vieitez, M. O., Tilstra, L. G., Tuinder, O. N. E., Koning, C. E., and Veefkind, J. P.: Evaluation of the operational Aerosol Layer Height retrieval algorithm for Sentinel-5 Precursor: application to Oxygen A band observations from GOME-2A, Atmospheric Measurement Techniques, 8, 4947–4977, https://doi.org/10.5194/amt-8-4947-2015, http://www.atmos-meas-tech.net/8/4947/2015/, 2015.

Sanghavi, S., Martonchik, J. V., Landgraf, J., and Platt, U.: Retrieval of the optical depth and vertical distribution of particulate scatterers in the atmosphere using O_2 A- and B-band SCIAMACHY observations over Kanpur: a case study, Atmospheric Measurement Techniques, 5, 1099–1119, https://doi.org/10.5194/amt-5-1099-2012, http://www.atmos-meas-tech.net/5/1099/2012/, 2012.

Seidel, F. C. and Popp, C.: Critical surface albedo and its implications to aerosol remote sensing, Atmospheric Measurement Techniques, 5, 1653–1665, https://doi.org/10.5194/amt-5-1653-2012, http://www.atmos-meas-tech.net/5/1653/2012/, 2012.

Tilstra, L. G., Tuinder, O. N. E., Wang, P., and Stammes, P.: Surface reflectivity climatologies from UV to NIR determined from Earth observations by GOME-2 and SCIAMACHY: GOME-2 and SCIAMACHY surface reflectivity climatologies, Journal of Geophysical Research: Atmospheres, https://doi.org/10.1002/2016JD025940, http://doi.wiley.com/10.1002/2016JD025940, 2017.

Tran, H. and Hartmann, J.-M.: An improved O2 A band absorption model and its consequences for retrievals of photon paths and surface pressures, Journal of Geophysical Research: Atmospheres, 113, D18 104, https://doi.org/10.1029/2008JD010011, http://onlinelibrary.wiley.com/doi/10.1029/2008JD010011/abstract, 2008.

Tran, H., Boulet, C., and Hartmann, J.-M.: Line mixing and collision-induced absorption by oxygen in the A band: Laboratory measurements, model, and tools for atmospheric spectra computations, Journal of Geophysical Research, 111, https://doi.org/10.1029/2005JD006869, http://doi.wiley.com/10.1029/2005JD006869, 2006.

Veefkind, J. P., Aben, I., McMullan, K., Förster, H., de Vries, J., Otter, G., Claas, J., Eskes, H. J., de Haan, J. F., Kleipool, Q., van Weele, M., Hasekamp, O., Hoogeveen, R., Landgraf, J., Snel, R., Tol, P., Ingmann, P., Voors, R., Kruizinga, B., Vink, R., Visser, H., and Levelt, P. F.: TROPOMI on the ESA Sentinel-5 Precursor: A GMES mission for global observations of the atmospheric composition for climate, air quality and ozone layer applications, Remote Sensing of Environment, 120, 70–83, https://doi.org/10.1016/j.rse.2011.09.027, http://www.sciencedirect.com/science/article/pii/S0034425712000661, 2012.

Winker, D. M., Vaughan, M. A., Omar, A., Hu, Y., Powell, K. A., Liu, Z., Hunt, W. H., and Young, S. A.: Overview of the CALIPSO Mission and CALIOP Data Processing Algorithms, Journal of Atmospheric and Oceanic Technology, 26, 2310–2323, https://doi.org/10.1175/2009JTECHA1281.1, http://journals.ametsoc.org/doi/abs/10.1175/2009JTECHA1281.1, 2009.

Witte, J. C., Douglass, A. R., da Silva, A., Torres, O., Levy, R., and Duncan, B. N.: NASA A-Train and Terra observations of the 2010 Russian wildfires, Atmospheric Chemistry and Physics, 11, 9287–9301, https://doi.org/10.5194/acp-11-9287-2011, http://www.atmos-chem-phys.net/11/9287/2011/, 2011.